Received: 9 December 2016 | Accepted: 22 August 2017
DOI: 10.1002/hyp.11346

WILEY

RESEARCH ARTICLE

# A modelling framework to simulate field-scale nitrate response and transport during snowmelt: The WINTRA model

Diogo Costa[1,3] | Jennifer Roste[1] | John Pomeroy[1,3] | Helen Baulch[2,3] | Jane Elliott[3,4] | Howard Wheater[2,3] | Cherie Westbrook[3,5]

[1]Centre for Hydrology, University of Saskatchewan, Saskatoon, SK, Canada
[2]School of Environment and Sustainability, University of Saskatchewan, Saskatoon, SK, Canada
[3]Global Institute for Water Security, University of Saskatchewan, Saskatoon, SK, Canada
[4]Environment and Climate Change Canada, National Hydrology Research Centre, Saskatoon, SK, Canada
[5]Planning, University of Saskatchewan, Saskatoon, Saskatchewan

**Correspondence**
Diogo Costa, Centre for Hydrology, University of Saskatchewan, Saskatoon, SK, Canada.
Email: diogo.costa@usask.ca

**Funding information**
Canada Excellence Research Chair in Water Security; Canada Research Chair in Water Resources and Climate Change; Canadian Water Network and the Natural Sciences and Engineering Research Council (NSERC), Grant/Award Number: 463960-2015

## Abstract

Modelling nutrient transport during snowmelt in cold regions remains a major scientific challenge. A key limitation of existing nutrient models for application in cold regions is the inadequate representation of snowmelt, including hydrological and biogeochemical processes. This brief period can account for more than 80% of the total annual surface runoff in the Canadian Prairies and Northern Canada and processes such as atmospheric deposition, overwinter redistribution of snow, ion exclusion from snow crystals, frozen soils, and snow-covered area depletion during melt influence the distribution and release of snow and soil nutrients, thus affecting the timing and magnitude of snowmelt runoff nutrient concentrations.

Research in cold regions suggests that nitrate ($NO_3$) runoff at the field-scale can be divided into 5 phases during snowmelt. In the first phase, water and ions originating from ion-rich snow layers travel and diffuse through the snowpack. This process causes ion concentrations in runoff to gradually increase. The second phase occurs when this snow ion meltwater front has reached the bottom of the snowpack and forms runoff to the edge-of-the-field. During the third and fourth phases, the main source of $NO_3$ transitions from the snowpack to the soil. Finally, the fifth and last phase occurs when the snow has completely melted, and the thawing soil becomes the main source of $NO_3$ to the stream.

In this research, a process-based model was developed to simulate hourly export based on this 5-phase approach. Results from an application in the Red River Basin of southern Manitoba, Canada, shows that the model can adequately capture the dynamics and rapid changes of $NO_3$ concentrations during this period at relevant temporal resolutions. This is a significant achievement to advance the current nutrient modelling paradigm in cold climates, which is generally limited to satisfactory results at monthly or annual resolutions. The approach can inform catchment-scale nutrient models to improve simulation of this critical snowmelt period.

**KEYWORDS**
agriculture, nitrate, nutrient exports, nutrient model, snow, winter

## 1 | INTRODUCTION

The prediction of runoff concentrations and nutrient exports from agricultural areas is still a major challenge despite decades of research on nutrient transport in watersheds. In the case of cold regions, progress has been made over the years to unveil the complex interplay between hydrological, chemical, and biological processes, but much remains to be understood. Phenomena such as (a) freeze-thaw cycling, (b) variable precipitation phases, that is, rainfall and snowfall, (c) rain-on-snow, and (d) runoff over frozen and unfrozen soils play an important role in the transport and fate of nutrients in cold regions watersheds but are poorly understood (Han, Xu, Liu, & Lian, 2010) and are often neglected or underrepresented in models. Other processes such as wind redistribution of snow and variable contributing areas in low relief landscapes, which are critical for instance in the Canadian Prairies in North America (Pomeroy, Davies, & Tranter, 1991; Spence et al., 2010), can also significantly impact the movement and storage of nutrients in the watershed.

In many cold regions, a significant portion of the annual nutrient load to rivers and lakes originates from agricultural land and occurs during

[Correction added on 17 January 2018, after the first online publication: e-mail of the corresponding author has been updated on this version.]

the major snowmelt event in spring (Bourne, Armstrong, & Jones, 2002), which is often the dominant runoff event of the year (Glozier, Elliott, Holliday, Yarotski, & Harker, 2006; Hansen, Sharpley, & Lemunyon, 2002; Liu, Elliott, Lobb, Flaten, & Yarotski, 2013; Nicholaichuk, 1967)—spring freshet can account for as much as 80% of the annual runoff in prairie environments (Gray, Norum, & Dyck, 1970). The spring snowmelt period is similarly important for nutrient export, transporting the majority of annual phosphorus and nitrogen loads—with more than 80% of transport occurring during this relatively short period (Baulch, Elliott, Wilson, Cordeiro, & Flaten, submitted). During this time, snow, soil, and surface residues are sources of nutrients, but the mechanisms and sequence by which these nutrients are released and transported are affected by the transient nature of snowmelt processes. Initially, the snowpack is the primary source of nutrients, but the soil becomes increasingly important as melt progresses due to soil frost and basal ice thawing increasing the contact between runoff and the soil matrix (Quinton & Pomeroy, 2006).

Heterogeneous snow accumulation and ablation cause the formation of a mosaic of thawing snow and growing "bare" soil patches as the snow-covered area declines during melt (Pomeroy et al., 1998), which affect the contributing area for runoff generation and the temporal pattern of nutrient release. This may have large implications for the time–space distribution of nutrient loads to rivers and lakes. Other processes such as atmospheric deposition, snow metamorphism, freeze-thaw cycles, and preferential ion exclusion also alter the spatial arrangement of ions in premelt snow covers (Davies et al., 1987; Johannessen & Henriksen, 1978). Some ions tend to be excluded over the winter to more mobile quasi-liquid layers between and around snow grains due to their lower ability to form hydrogen bonds and incorporate the ice crystal lattice during thaw-freeze cycles (Lilbæk & Pomeroy, 2008). This results in these ions readily mixing with percolating meltwater, causing ionic pulses in early snowmelt runoff (Colbeck, 1981, 1987).

Some models, such as Spatially referenced regressions on watershed attributes (Douglas-Mankin, Srinivasan, & Arnold, 2010; Wellen, Arhonditsis, Labencki, & Boyd, 2014) have been widely applied in cold regions in North America to statistically estimate the relationship between stream concentrations and sources/sinks of nutrients. However, these estimates are purely empirical, which makes such models less suitable for predictive studies and basic research on the mechanisms of nutrient [including nitrate ($NO_3$)] release and transport during snowmelt.

Popular process-based models have also been used in the context of cold climates, such as Hydrological predictions for the environment (Arheimer, Dahné, Donnelly, Lindström, & Strömqvist, 2012; Lindstrm, Pers, Rosberg, Strömqvist, & Arheimer, 2010), Hydrological simulation Program–Fortran (Bicknell, Imhoff, Kittle Jr., Donigan Jr., & Johanson, 1997; Duda, Hummel, Donigian Jr., & Imhoff, 2012), Integrated Model of Nitrogen in Catchments (Arnold et al., 2012; Futter et al., 2012; Wade, Whitehead, & O'Shea, 2002; Whitehead, Wilson, Butterfield, & Seed, 1998, 1998), and SWAT (Soil and Water Assessment Tool; Borah & Bera, 2003). Even so, these models have been primarily applied to areas where rainfall-runoff processes and unfrozen soils are still dominant, and tests in regions with long cold winters and seasonal snow cover are rare. Therefore, there has been limited critical evaluation of the performance of the models in such environments and the role of cold region processes in these model applications. In addition, a closer look at the representation of snow processes in these models, particularly those affecting nutrient transport, reinforces the need for enhancement of model algorithms for use in cold climates.

In areas with seasonal snow cover, the transport of nutrients is strongly influenced by snow accumulation, runoff, and infiltration over frozen or partially frozen soils and freeze-thaw cycles (Pomeroy et al., 2007). Subdaily simulation time steps are often required for hydrological applications (Tobin et al., 2013) and, in cold climates, this is particularly necessary for adequate representation of blowing snow redistribution, snow-covered area depletion during snowmelt, meltwater ionic pulses, high magnitude-low frequency rain events, and individual flowpaths to streams. Most process-based models are run, or predictions reported and compared with observations at daily, weekly, or monthly time intervals (Wellen, Kamran-Disfani, & Arhonditsis, 2015). This is in part due to model predictions often improving for monthly and annual runoff balances, as reported in various studies (e.g., Arnold, Muttiah, Srinivasan, & Allen, 2000; Shirmohammadi, Chu, Montas, & Sohrabi, 2001; Wang, A. M., & Melesse, 2005) and due to the inability of many of these models to adequately simulate rapid hydrological changes, such as caused by flood events (Arnold, Srinivasan, Muttiah, & Williams, 1998; Borah & Bera, 2003). Due to the rapid (episodic) nature of snowmelt, a shorter time step is hence important to capture correctly the movement of water and transport of nutrients (Borah & Bera, 2003) during this period.

In all models examined, the release and transport mechanisms during snowmelt and rainfall-runoff events are undifferentiated. However, numerous field studies have shown that nutrient losses from snowmelt-induced and rainfall-induced runoff are different in many ways. Snowmelt runoff carries a greater nutrient load due to reduced infiltration rates, large runoff volumes (Li, Elliott, & Tiessen, 2011), and cold temperatures limiting biological uptake (Rattan et al., 2017), but mainly in the dissolved form (Cade-Menun et al., 2013) due to frozen soils restricting particle detachment (Panuska & Karthikeyan, 2008). Consequently, concentrations of nutrients during snowmelt are typically higher than during rainfall-runoff events (Rattan et al., 2017). During this period, the mixing of runoff with soil-pore water and nutrients is affected by soil frost and uneven snow-cover depletion, leading to the formation of mosaics of snow and bare soil patches (Pomeroy et al., 1998), which affects the contributing sources and areas. Some models, such as Hydrological Predictions for the Environment and SWAT, use fractional areal snow-cover depletion curves to account for the effect of this phenomena on the geometry, area, energetics, and melt of the snowpack (Pomeroy et al., 1998), but these calculations have not been extended to the nutrient calculations. Consideration of snow- cover depletion is important for explicit representation of discontinuities in nutrient supply (i.e., snow and soil-pore water), which is a necessary step for adequate simulation of timings and magnitudes of concentration peaks at temporal resolutions that are compatible/relevant to the process of snowmelt (e.g., hourly).

A major challenge in cold climate hydrochemistry is the adequate simulation of solute transport, that is, the hydrological drivers. Winter conditions (e.g., temperature, snowfall, and blowing snow) greatly affect many hydrological processes (e.g., snow accumulation, snowmelt, infiltration, and blowing snow; Pomeroy et al., 2007), influencing nutrient export to streams (e.g., Brooks & Williams, 1999; Casson, Eimers, & Watmough, 2012; Eimers, Watmough, Paterson, Dillon, & Yao, 2009). Therefore, improvements to existing models are crucial for superior background hydrological/transport simulations. Some of the limitations found in existing models include the use of the empirical temperature-index method (Arnold et al., 1998), which requires model recalibration whenever used with new regional climatic inputs (Fuka et al., 2012) or during the melt season, the absence of blowing snow redistribution and sublimation modules (Pomeroy et al., 1998) and the inadequate simulation of runoff over frozen or partially frozen soils (Han et al., 2010). Blowing snow and sublimation, for instance, can cause −40% to +100% changes in the spatial distribution of snow in prairie and arctic regions (Pomeroy et al., 1998).

Some recent improvements to existing nutrient models for application to cold environments are noteworthy, particularly for SWAT. The nitrate module of SWAT was enhanced for simulation of a Canadian Shield catchment by incorporating dynamic nitrogen deposition and by enabling its quick mobilization by macropore flows (Zhang, Chen, & Yao, 2016). Mekonnen, Mazurek, and Putz (2016) developed SWAT-PDLD (probability distributed landscape depressions) for simulation of prairie watersheds based on Shook and Pomeroy (2011) paradigm (denoted as Model 1) whereby probability distributions function are incorporated to represent wetland complexes. A varying soil erodibility factor was also introduced to account for seasonal changes in nutrient and sediment release due to cold climate conditions (Mekonnen, Mazurek, & Putz, 2017). Unfortunately, despite these important advances, SWAT required intense parameter calibrations and showed high model uncertainty and equifinality phenomena. This is a common problem for most conceptual nutrient models due to heavy parameterization, in the sense that the parameters are not normally identifiable from available data (McIntyre, Jackson, Wade, Butterfield, & Wheater, 2005). These models were run at daily time steps, and, to the knowledge of the authors, no other attempts (or model developments) have been made to improve the temporal resolution (i.e., subdaily) and overall process representation of the particular snowmelt event, a short but critical period for nutrient transport. This suggests the need for continuous improvement of models and the strong role of process-based models that build on the availability of supporting data. Such models are critical to advance the current available modelling capability and allow for more physically based and efficient parameterizations.

In this research, a process-based nutrient model for hourly estimates of runoff $NO_3$ concentrations was developed based on the simulation of the key snow-soil $NO_3$ release, transport, and migration mechanisms controlling field-scale diffuse loading/export during snowmelt.

## 2 | MATERIALS AND METHODS

### 2.1 | Review of critical processes

Nutrients from agricultural land are transported to streams and lakes mainly through runoff (Liu et al., 2013). In cold regions, the dominant runoff event of the year is often snowmelt-induced (Hansen, Gupta, & Moncrief, 2000), but many other natural and anthropogenic factors such as soil properties, hydrological and weather conditions (Shrestha, Dibike, & Prowse, 2012; Townsend-Small, McClelland, Max Holmes, & Peterson, 2011), and agricultural practices (Steinheimer, Scoggin, & Kramer, 1998) can affect the amount of nutrients that are effectively lost to runoff each year.

Runoff $NO_3$ concentrations vary significantly during snowmelt (e.g., Brunet & Westbrook, 2012) due to discontinuities in nutrient supply. These are caused by changes in the sources, the transport and transformation mechanisms, and other physical factors (Liu et al., 2013). Simultaneously, higher portions of dissolved total N and P are associated with this period due to snowmelt runoff being generally less erosive than most runoff produced by rainfall (Cade-Menun et al., 2013).

$NO_3$ is highly soluble in water and exists in soil mostly in pore water. Thus, it is easily transported through runoff or below the plant-rooting zone (Piatek, Mitchell, Silva, & Kendall, 2005), potentially also affecting groundwater. $NO_3$ is negatively charged, so it is not retained by the soil particles (Martius, Rudenko, Lamers, & Vlek, 2011) like other nutrients, such as ammonium ($NH_4$). Heterotrophic microbiological activity occurs during snowmelt (Brooks, Williams, & Schmidt, 1996; Clark, Chantigny, Angers, Rochette, & Parent, 2009), but has also been observed in snow-covered soils during winter (Brooks et al., 1996; Clark et al., 2009; Pellerin et al., 2012; Sebestyen et al., 2008; Snider, Wagner-Riddle, & Spoelstra, 2017). Net mineralization and nitrification may occur in frozen soils before snowmelt (Brooks et al., 1996; Clark et al., 2009), therefore presenting a risk of $NO_3$ net gains between fall and spring, particularly in the presence of organic amendments and in fine-textured soils (Clark et al., 2009).

However, nitrification and the flushing of surficial soil $NO_3$ during snowmelt rapidly decreases $NO_3$ concentrations (Petrone, Buffam, & Laudon, 2007; Sebestyen et al., 2008), particularly in late snowmelt. In early snowmelt, chemical species may be considered conservative depending on the rapid nature of transport (Pomeroy, Jones, Tranter, & Lilbæk, 2006; Sebestyen et al., 2008) and on snow cover and soil frost limiting interactions between meltwater and the soil (Deelstra et al., 2009; Marsh & Pomeroy, 1999). This is classically assumed to be a period of low biological uptake due to low temperatures, frozen soils, and lack of vegetative growth (Clark et al., 2009; Petrone et al., 2007; Tiessen et al., 2010). Biological activity in melting snow can occur, but it may only be significant when snowmelt is slow and provides longer exposure to free water for algae life cycles (Tranter & Jones, 2001). In spite of that, ionic pulses in early snowmelt runoff may still occur, (Davies et al., 1987; Han et al., 2010; Johannessen & Henriksen, 1978), a phenomenon that has been observed for most anions and cations, including $NO_3$, and has been linked to atmospheric deposition and ion exclusion to the air–ice interface during ice recrystallization (e.g., Bales, Davis, & Stanley, 1989; Williams & Melack, 1991; Wren & Donaldson, 2011).

During winter, solutes in the snow matrix fractionate due to repeated cycles of snow densification (metamorphism) and refreezing of meltwater causing the preferential segregation of ions (Davis, 1991; Pomeroy et al., 2006); ions migrate from the ice crystal lattice to the surface of the snow grain. This accumulation of ions forms quasi-liquid layers surrounding snow grains (Colbeck, 1981, 1987), the freezing point of which declines due to increasing salt concentrations, resulting in the rapid mobilization of a major portion of snow ions with the first meltwater (Colbeck, 1981; Johannessen & Henriksen, 1978). This process is commonly referred to as "solute leaching from snow grains." Stein, Proulx, and Lévesque (1994) observed further that when a period of extreme cold is followed by melt, the meltwater may refreeze when entering the deeper cold snow and promote the layering of solutes in the snowpack, increasing the magnitude of the ionic pulses in early meltwater (Bales et al., 1989; Williams & Melack, 1991). This process has been observed both in laboratory and field experiments (e.g., Colbeck, 1981; Marsh & Pomeroy, 1999). Meyer and Wania (2008) added that contaminant/nutrient shock loads are more likely during melt-runoff events over frozen soils when in the presence of permeable soils. Two independent lab experiments conducted by Lilbæk and Pomeroy (2008) and Hodson (2006) observed that the formation of a basal ice layer over saturated or very cold frozen soils can enrich initial meltwater ion concentrations, including $NO_3$, with the latter study suggesting a concentration factor (CF, ratio between early meltwater peak and bulk snow water concentrations) in the range of 23 to 39. Other phenomena such as rain-on-snow, variable contributing areas, and freeze-thaw cycles may also affect the timing and magnitude of the annual nutrient load in agricultural areas. Increased frequency of rain-on-snow events, for instance, has been associated with warmer winters and observed to release significant amounts of snow and soil nutrients rapidly to runoff before the main spring freshet (e.g., Casson et al., 2012; Groffman et al., 2001; Jones, 1999).

The impact of nutrient leaching from the ground cover, litter, and upper soil horizons on meltwater chemistry is widely controlled by the patchiness of the disintegrating snow cover (Pomeroy et al., 1998) and of the eroding concrete frost (Deelstra et al., 2009; Jones & Pomeroy, 2001; Sebestyen et al., 2008), which increases as melt progresses. Changes in meltwater $NO_3$ across diverse landscapes strongly depend on interactions of meltwater with the soil matrix and pore water and on dilution (e.g., Deelstra et al., 2009; Jones & Pomeroy, 2001; Quinton & Pomeroy, 2006). The fragmentation of the snowpack causes the development of a mosaic of thawing snow and growing bare soil patches (Pomeroy et al., 1998). This has effects on the contributing areas and sources of nutrients during melt; more pure snowpack meltwater in early runoff and more enriched soil-pore water in later runoff. In a study on an Arctic forest-tundra site, Marsh and Pomeroy (1996) showed, for example, that during this period small-scale lateral sensible heat fluxes from bare patches to snow-covered areas exacerbate the heterogeneous snowmelt pattern. This has implications for runoff-soil interactions with possible anticipation of the timing of the first and major surficial soil $NO_3$ flush. As the water moves downstream, runoff $NO_3$ concentrations tend to decrease due to biological assimilation and denitrification, even in agricultural areas (Snider et al., 2017). However, at the spatial scales of nutrient release and mobilization (i.e., field-scales), the spatial distribution of snow mass and melt rate are critical determinants of the spatial and temporal dynamics of $NO_3$ export.

Conservation tillage (i.e., zero-till, minimum tillage, incomplete tillage, and reduced tillage) has been widely promoted as a beneficial management practice for reduction of sediment and nutrient loading (Lal, 2003) via soil erosion control and increase of soil porosity and infiltration (Lipiec, Kuś, Słowińska-Jurkiewicz, & Nosalewicz, 2006) Tillage can affect the wind redistribution of snow and has been linked to decreased soil water content and increased runoff and erosion. However, both positive and adverse effects on nutrient exports have been reported in the literature, discrepancies that have been attributed to differences in climate and topography (Tiessen et al., 2010).

Widespread adoption of conservation tillage on the prairie has the impact of leaving stubble or plant residue on the soil surface. This plant residue can release nutrients to runoff, particularly phosphorus (P), depending on various factors, such as the plant nutrient content (Miller, Beauchamp, & Lauzon, 1994) and cell rupture caused by freeze-thaw cycles during winter (e.g., Bechmann, Kleinman, Sharpley, & Saporito, 2005; Messiga, Ziadi, Morel, & Parent, 2010). Because the focus of this study is $NO_3$, plant residue is typically relatively small when compared to other sources (Elliott, 2013), and thus, it is neglected. In the case of $NH_4$, plant residue and vegetation can be a major source and even greater than the soil (Elliott, 2013). Fertilizers are important sources of nutrients and have been linked to increased runoff nutrient loads (e.g., Buda & Kleinman, 2009; Moog & Whiting, 2002) or runoff nutrient concentrations (e.g., Elliott, Cessna, & Hilliard, 2001; Liu et al., 2013) and cannot be ignored.

## 2.2 | Modelling approach

The goal of this study is to improve the modelling of field $NO_3$ mobilization, diffuse loading, and transport from prairie agricultural land (i.e., field-scale) for improved nutrient export estimations in cold regions. This is accomplished by combining different process-based algorithms for explicit representation of snow and soil $NO_3$ processes into a new stand-alone model and by coupling it to the Cold Regions Hydrological Model (CRHM) for adequate simulation of transport/hydrological processes. These simulation algorithms were developed based on a conceptual model that was created to encapsulate the main $NO_3$ release and transport processes discussed in Sections 1 and 2.1.

Figure 1 shows the conceptual model from which the numerical model was developed. It considers five distinct phases regarding the dominant processes affecting runoff concentrations. *Phase 1* is the initial period when snow begins to melt. Wetting fronts start to move vertically through the snowpack, possibly forming preferential flows (i.e., flow fingers) and eventually infiltrating or refreezing (Marsh & Woo, 1984). According to Marsh and Woo, this causes the growth of ice layers and retards the advancement of the wetting front and the arrival of meltwater. Ions accumulate during winter at the air–water interface and in quasi-liquid layers due to ion exclusion (i.e., leads to high salt concentrations thus lowers the freezing point) and at the snow–air interface due to atmospheric deposition. As a result, the wetting front is accompanied by an ion front. Evidence of this phenomenon has been observed in meltwater, and Marsh and Pomeroy (1999) attribute this concentration rise to the load being less diluted, which is consistent with the hypothesis used here of an ion front eventually reaching the stream.

In *Phase 2*, the snow ion wavefront reaches the edge-of-the-field (EOF) and ion concentrations peak (including $NO_3$). *Phase 3* is a transition period characterized by a decline in concentrations as the ion-rich snow layers (top snow and quasi-liquid layers within the snowpack) become progressively depleted. During this period, the remaining snow (i.e., ion-poor) becomes the main source of ions. The formation of these ion-poor lower layers is another consequence of the vertical redistribution of ions during winter via ion exclusion (e.g., Lilbæk &

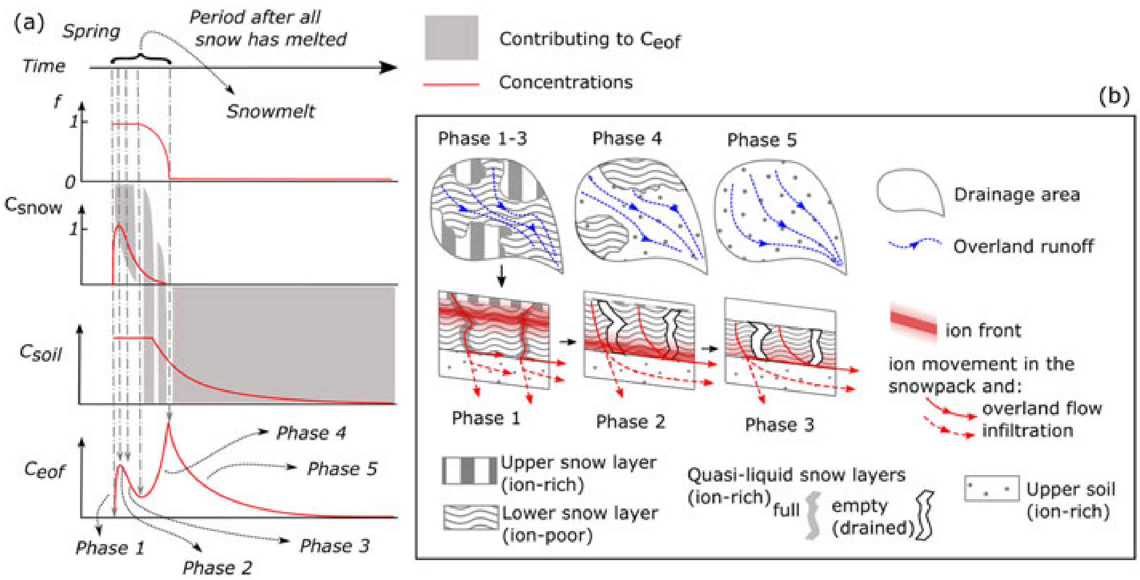


**FIGURE 1** Conceptual model framework. (a) Snow, soil, and edge-of-the-field ion concentrations during snowmelt. *f* Is the snow- cover fraction and $c_{snow}$, $c_{soil}$, and $c_{EOF}$ are snow, soil, and edge-of-the–field concentrations, respectively. (b) Schematic representation of the contributing areas and vertical solute transport during each transport phase

Pomeroy, 2010). Although ions within the snowpack migrate to form ion-rich layers, the remaining layers became ion-poor, have a higher freezing point, and melt later. In *Phase 4*, which is also a transitional period, ions in the upper soil water solution begin to mix with runoff as soil-runoff interactions increase with the growing bare soil patches. Finally, *Phase 5* occurs when the only source of ions is the soil and the accumulated plant residue. The leaching of $NO_3$ from plant residue is typically relatively small when compared to other sources (Elliott, 2013), and thus, it is ignored in the simulations. Through this phase, soil $NO_3$ is transported during late snowmelt via flushing, and soil $NO_3$ losses occur via biotic uptake, which would be dominated by denitrification rather than assimilation. This leads to the depletion of readily available soil $NO_3$ as snowmelt progresses, causing runoff concentrations to decrease. The model relies on the following assumptions for purposes of simplifying this first model version validation:

1. Winter: Transformations between fall and spring are negligible due to low plant uptake and microbiological activity; and
2. Early snowmelt: Assimilation, denitrification, or flushing of surficial soil via runoff are negligible due to the snow cover and soil frost limiting runoff-soil contact.

The scope of this model is the field-scale nutrient release process and the duration of the snowmelt period; however, the five-phase methodology presented can be extended to larger scale simulations. At large scales, however, damping of concentration pulses is expected to occur via dilution, routing, and lack of synchronicity as runoff water moves through the river network, and in-stream processes may grow increasingly important (e.g., Petrone et al., 2007).

## 2.3 | Model development

The new model, named WINTRA (Winter Nutrient field Transport), has its origins in the Roste, (2015) paradigm. It is modular, with each model component developed to simulate separate processes and facilitate the continuous improvement of the model. WINTRA uses simulation outputs from hydrological models created using the CRHM platform (Fang et al., 2013; Mahmood, Pomeroy, Wheater, & Baulch, 2016; Pomeroy et al., 2007) as the baseline hydrological driver. CRHM is a flexible, modular numerical model framework developed around the concept of hydrological response units (HRU), which are used to represent distinct landscape elements. These landscape elements are defined based on the dominant transport processes, which can include blowing snow, overland flow, organic layer subsurface flow, mineral interflow, groundwater flow, and streamflow.

CRHM integrates several algorithms to account for hydrological processes that are unique to cold regions, including some specific to the Canadian Prairies, such as wind redistribution of snow during winter (e.g., Pomeroy & Jones, 1996) and variable contributing areas (e.g., Spence et al., 2009). Contrary to most hydrological models, including some of those discussed in Section 1, CRHM runs at hourly time steps. This is a critical feature for regions like the Canadian Prairies, where spring snowmelt runoff typically occurs during a short period (i.e., 1–3 weeks), accounts for more than 80% of the annual runoff volume (Gray & Landine, 1988) and contributes most of the P and N exported annually (Corriveau, Chambers, & Culp, 2013). Using hourly temperature and precipitation data enables CRHM to better capture water and nutrient pulses during spring snowmelt events and other phenomena such as the rapid decrease in soil infiltrability due to the formation of ice lenses. Besides successful deployment in Canada, CRHM has been suitably used in other cold regions such as the Tibetan Plateau (Zou, Zhu, Zhou, Li, & Ma, 2014), Svalbard (López-Moreno, Boike, Sanchez-Lorenzo, & Pomeroy, 2016); Patagonia (Krogh et al., 2015); US north-west (Rasouli, Pomeroy, & Marks, 2015); Alps (Weber et al., 2016), and Pyrenees (López-Moreno et al., 2014).

**FIGURE 2** Wheat stubble near Rosthern, Saskatchewan during snowmelt in 2016. Courtesy of Phillip Harder

The WINTRA model was developed based on a field-based solute mass balance that includes snow and soil water:

$$(V_{eof} + V_{inf}) \cdot c_{eof} = V_{snow} \cdot c_{snow} + V_{soil} \cdot c_{soil}, \tag{1}$$

where $c$ are concentrations $[ML^3]$, $V$ are runoff volumes $[L^3T]$, and the subscripts "eof," "inf," and "soil" are used to refer to EOF, infiltration, and soil, respectively. It is assumed that the concentration of solute in EOF runoff and infiltration water is the same. The volume $V_{eof} + V_{inf}$ represents the total snowmelt runoff volume ($V_{melt}$). $V_{soil}$, and $V_{snow}$ are the fractions of snowmelt runoff that originate from the snowpack and frozen soil-pore water, respectively.

Runoff volumes ($V_{melt}$) originate from the snowpack ($V_{snow}$) and/or soil-pore water ($V_{soil}$) depending on the varying areal fractions of the melting bare soil water and snow. This is represented in the model by computing snow-cover areal curves (see example in Figure 2). This approach allows reducing the number of variables in Equation 1, which can be rearranged as:

$$c_{EOF_t} = f \cdot c_{snow} + (1 - f) \cdot c_{soil}, \tag{2}$$

where $f$ [-] represents the snow-cover fraction during melt ($\cong V_{snow}/V_{melt}$). $f$ Values are calculated from snow-cover depletion curves (Essery & Pomeroy, 2004). In winter, heterogeneous snow-cover surfaces form due to the action of wind and variable land roughness (e.g., vegetation). During melt in spring, these nonuniform snowpacks are reduced to patchy snow-covered areas before all snow has disintegrated and disappeared (see example in Figure 2). The snow-cover fraction ($f$) characterizes this phenomenon, and the formulation developed by Essery and Pomeroy (2004) is used as the model,

$$f = tanh\left(1.26\frac{SWE_t}{\sigma_0}\right), \tag{3}$$

where $SWE_t$ (millimetre) is the snow water equivalent and $\sigma_0$ (millimetre) is the premelt $SWE$ standard deviation (millimetre). Figure 3 depicts the relationship provided in Equation 3 to highlight that the soil remains fully covered in snow ($f = 1$) during a significant portion of the initial snowmelt period (Phases 1–3, Figure 1). During this period, that is, $f = 1$, it is assumed that $NO_3$ in soil-pore water remains immobile and the snow is the only source of $NO_3$ to runoff. This has strong implications for soil-runoff interactions and is critical for accurately simulating the timing of the second pulse (Phase 4, maximum soil nutrient diffusive load).

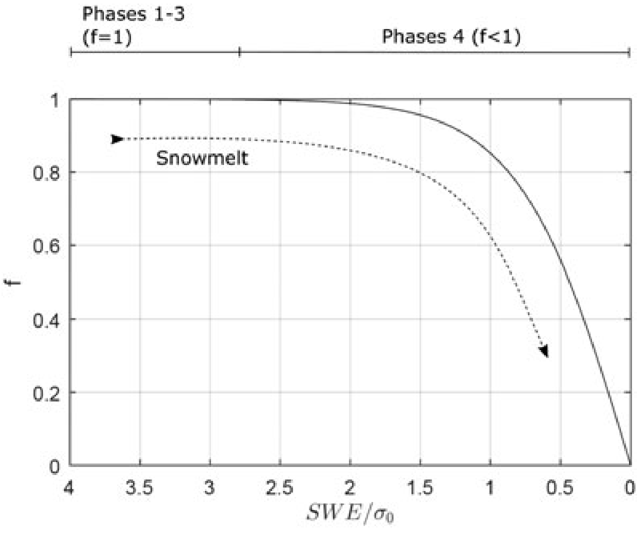


**FIGURE 3** Relationship between fractional covered area (f) and $SWE/\sigma_0$ during melt (from Equation 3, Essery & Pomeroy, 2004). Phases 1–4, which are related to the conceptual model depicted in Figure 1, are highlighted

To account for the transport of $NO_3$ in the periods during and after melt ($f \neq 0$ and $f = 0$, respectively), Equation 2 was extended to a piecewise function:

$$c_{eof_t} = \begin{cases} f_t \cdot c_{snow_t} + (1 - f_t) \cdot c_{soil_t}, & \text{during snowmelt} \\ c_{soil_t}, & \text{SWE} = 0 \end{cases} \tag{4}$$

where $c_{snow}$, $c_{soil}$, and $c_{eof}$ are snow, soil-pore water, and runoff (EOF) $NO_3$ concentrations. During the period after all snow has melted, it is assumed that runoff can freely interact with the soil. The amount of $NO_3$ in the pore soil water readily available for runoff transport is modelled using Equations 5 and 6:

$$c_{soil_t} = c_{soil_{t-1}} - \partial c / \partial t \quad (5)$$

$$\frac{\partial c}{\partial t} = \begin{cases} k_d \cdot c_{soil_{t-1}}, & SWE = 0 \\ 0, & SWE > 0 \end{cases} \quad (6)$$

where $k_d$ $[T^{-1}]$ is the depletion rate of readily available soil-pore water $NO_3$ via assimilation, denitrification, leaching, or flushing of surficial soil via runoff. These processes are approximated/simplified as a first-order elimination process (exponential decay) that depends on the evolution of soil $NO_3$.

The effect of ion exclusion in $c_{snow}$ is simulated using the *CF* concept first introduced by Johannessen and Henriksen (1978) based on observations at a Norwegian catchment. This concept was later extended by others to different cold regions (e.g., Lilbaek, 2007; Stein, Jones, Roberge, & Sochanska, 1986; Tranter et al., 1986). *CF* relates meltwater concentrations ($c_{snow}$) with snow-cover concentrations measured at the onset of melt ($c_{snowpack}$) as

$$c_{snow} = CF \cdot c_{snowpack}. \quad (7)$$

Recall that $c_{snow}$ is used to refer to meltwater originating from the snowpack before interaction with the soil. *CF* is calculated based on *SWE* dynamics using Stein et al. (1986) expression,

$$CF_t = \frac{1}{\bar{M}} \cdot \frac{d}{dt}\left((SWE_t - \bar{M} \cdot t) \cdot e^{-k_l \cdot \bar{M} \cdot t}\right), \quad (8)$$

where $t$ is the time from the start of melt, *SWE* is the premelt snow water equivalent, $\bar{M}$ is the average melt rate for the whole melt period, and $k_l$ is a dimensionless leaching coefficient.

The model uses premelt snow and fall soil $NO_3$ concentrations as model inputs, alongside with air temperature, precipitation, relative humidity, and wind speed for the estimation of the transport processes by the hydrological model component (CRHM), which is externally coupled to WINTRA. The soil-pore water $NO_3$ concentrations used to initiate the model ($c_{soil_{t0}}$, Equation 5) are reset annually based on hydrological years and using observations taken in the fall each year. This allowed to include the effect on the premelt surficial soil $NO_3$ pool of unused fertilizer applied during the growing season or in the fall of the preceding year). Although a substantial amount of observation data is required to run the model, the approach adopted aims to reduce model uncertainties associated with high number of calibrated parameters and establish a snowmelt model structure that can be linked to soil models.

### 2.3.1 | Field data and model application

The Steppler watershed, South Tobacco Creek basin, in Manitoba, Canada, was used as a test bed to evaluate the coupled CRHM and WINTRA models (Figure 4). The set-up and validation of the model results were supported by 3 years of high-frequency field-scale data measured at six agricultural fields in this subbasin. Such highly resolved time series are necessary for adequately capturing the timing, magnitude, and rate of nutrient release and transport during snowmelt (Pellerin et al., 2012; Steinheimer et al., 1998).

The location of the case study is strategic for the study of nutrient runoff from agricultural land as these are subbasins of the Red River watershed, which contributes more than half of the nutrient load to Lake Winnipeg (LWST, 2009). The water quality of this lake has

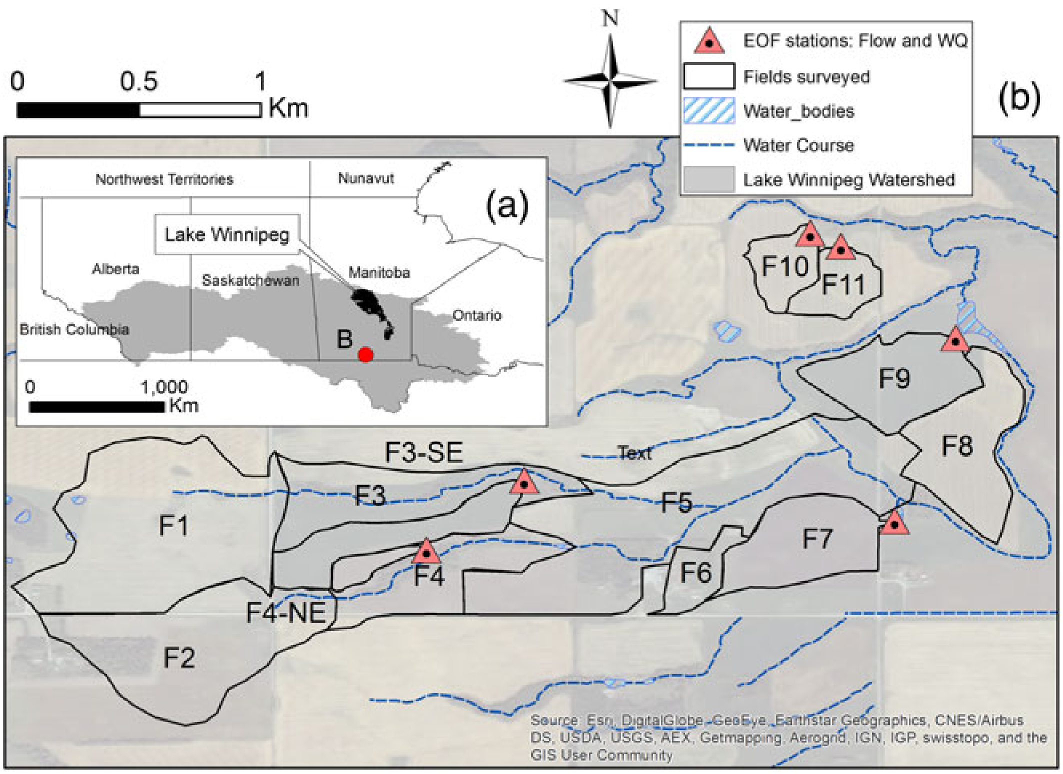


**FIGURE 4** (a) Location of the Stepper Catchment, a subbasin of the Lake Winnipeg Watershed, Canada. (b) Fields surveyed and the location of the discharge and water quality monitoring stations

**TABLE 1** Agricultural records at Steppler Basin

| Field (area [ha]) | Year | Tillage Fall | Tillage Spring | Crop seeded |
|---|---|---|---|---|
| F3 | 2009 | HDC | LDC+Harrow | Green feed oats |
| (8.33) | 2010 | No tillage | No tillage | Alfalfa/Timothy[a] |
| | 2011 | No tillage | No tillage | Alfalfa/Timothy[a] |
| F4 | 2009 | No tillage | No tillage | Alfalfa/Timothy |
| (2.45) | 2010 | HDC+LDC | LDC | Canola |
| | 2011 | HDC + Harrow | Anhydrous rig | Wheat |
| F7 | 2009 | No tillage | No tillage | Alfalfa/Timothy |
| (12.7) | 2010 | HDC +LDC | LDC | Wheat |
| | 2011 | HDC +Harrow | Anhydrous rig | Canola |
| F9 | 2009 | HDC | LDC+Harrow | Green feed oats |
| (10.2) | 2010 | No tillage | No tillage | Alfalfa/Timothy[a] |
| | 2011 | No tillage | No tillage | Alfalfa/Timothy[a] |
| F10 | 2009 | HDC | LDC+HDC | Wheat |
| (4.16) | 2010 | HDC | LDC | Canola |
| | 2011 | HDC | Anhydrous rig | Wheat |
| F11 | 2009 | No tillage | Harrow | Wheat |
| (5.15) | 2010 | HDC | No tillage | Canola |
| | 2011 | HDC | No tillage | Wheat |

*Note.* LDC and HDC refer to light and heavy duty cultivator, respectively (adapted from Roste 2015).
[a]Postharvest 2009.

significantly deteriorated due partially to excess nutrient load (e.g., Schindler, Hecky, & McCullough, 2012). It is the 10th largest in the world by surface area and is considered the most eutrophic among them (Voora & Venema, 2009). Cyanobacteria blooms have nearly doubled in size since the 1990s (Schindler et al., 2012), threatening its significant recreational and economic value (e.g., Ofukany, Hobson, Wassenaar, & Bond, 2015).

This region is characterized by subhumid continental climate, long and cold winters, and a mean annual precipitation of about 550 mm (ECCC, 2014). Around 70% of the annual runoff and nutrient losses from the South Tobacco Creek basin occur during snowmelt runoff (Glozier et al., 2006). The reader is referred to Li et al. (2011), Liu, Elliott, Lobb, Flaten, and Yarotski (2014), and Mahmood et al. (2016) for more information about this basin.

The Steppler watershed is crisscrossed by two intermittent water courses and has a drainage area of 205 ha that is divided into several fields used to grow different crops on a rotational basis (Li et al., 2011). Between 2009 and 2011, the soil was subject to different tillage and cropping practices. The crops seeded included cereal grains, green feed oats, alfalfa, and timothy grass (Table 1, adapted from Li et al., 2011 and Roste 2015).

During the surveyed period, runoff was constrained inside the basin by reinforcing natural watershed boundaries with soil berms. EOF flow rates were determined using circular flumes (Fields F3, F7, and F9) or compound angle v-notched weirs (Fields F4, F10, and F11), by means of water levels measured at 5–10 min intervals using ultrasonic sensors and data loggers (Liu et al., 2014; Roste, 2015; Tiessen et al., 2010). Such high-frequency measurements were important to capture flow peaks during both snowmelt and rainfall-runoff events. Water was sampled and tested for nitrate-nitrite ($NO_3 - NO_2$) during several snowmelt and rain runoff events using an auto-sampler and data logger (Liu et al., 2014; Roste, 2015; Tiessen et al., 2010). We assume the $NO_3 - NO_2$ is mainly composed of $NO_3$.

**TABLE 2** Summary of edge-of-the-field water level and water quality field measurements collected for each field by Agriculture and Agri-Food Canada and Environment Canada

| Field | Variable | Snowmelt events monitored 2008 | 2009 | 2010 | 2011 | No. Obs. |
|---|---|---|---|---|---|---|
| F3 | Water levels | | | x | x | 11,338[a] |
| | Premelt *SWE* | x | x | x | x | 4 |
| | $NO_3$ runoff conc. | | x | x | x | 48[b] |
| F4 | Water levels | | | x | x | 29,806[a] |
| | Premelt *SWE* | x | x | | x | 3 |
| | $NO_3$ runoff conc. | | x | x | x | 47[b] |
| F7 | Water levels | | x | x | x | 1,059[a] |
| | Premelt *SWE* | | | | | — |
| | $NO_3$ runoff conc. | | x | x | x | 44[b] |
| F9 | Water levels | | x | x | x | 9,010[a] |
| | Premelt *SWE* | | | | | 4 |
| | $NO_3$ runoff conc. | | x | x | x | 88[b] |
| F10 | Water levels | x | x | x | x | 15,985[a] |
| | Premelt *SWE* | x | x | x | x | 4 |
| | $NO_3$ runoff conc. | | x | x | x | 87 |
| F11 | Water levels | x | x | x | x | 14,800[a] |
| | Premelt *SWE* | x | x | x | x | 4 |
| | $NO_3$ runoff conc. | | x | x | x | 70 |

*Note.* This data set is used in Section 3 to verify the model performance.
[a]continuous measurements (5 min interval).
[b]samples collected during major runoff events.

**TABLE 3** Summary of the climate data measured at Twins basins and used to force the hydrological model

| Annual statistics | Hydrological year 2007–2008 | 2008–2009 | 2009–2010 | 2010–2011 |
|---|---|---|---|---|
| P [mm] | 721 | 778 | 789 | 723 |
| Mean T (Std T) [°C] | 2.8 (14.0) | 2.5 (14.5) | 4.6 (13.2) | 3.5 (14.6) |
| Mean RH (Std RH) [%] | 72.1 (18.3) | 74.4 (16.2) | 75.0 (18.7) | 75.2 (17.1) |
| Mean U (Std U) [m/s] | 4.9 (2.7) | 4.7 (2.8) | 4.4 (2.7) | 4.8 (2.8) |

*Note.* P, T, RH, and U refer to precipitation, air temperature, relative humidity, and wind velocity, respectively. Std refers to standard deviation.

The experimental set-up aimed to capture subdaily $NO_3$ concentrations and load dynamics during the rising, peak, and falling limb of the snowmelt hydrographs, an aspect that was critical for the adequate validation of hourly model outputs. Table 2 summarizes the collected data, which were used to verify the performance of both the hydrological and nutrient model components.

Precipitation (*P*), air temperature (*T*), relative humidity (*RH*), and wind speed (*U*) were measured locally at 5-min intervals and upscaled to hourly time steps to force CRHM. Table 3 provides a summary of the climate data used. The accurate simulation of *SWE* in CRHM is extremely important because it is used in WINTRA to compute both *CF*, Equation 8), and areal snow-cover fraction curves (*f*, Equation 3). The calculation of *f* requires standard deviation estimates of *SWE* ($\sigma_{SWE}$) to account for the effect of premelt snow-cover heterogeneities on the geometry and area of the snow cover as it disintegrates during ablation (Pomeroy et al., 1998). In this study, peak snow depth and density, which are used to calculate *SWE*, were both measured annually at the onset of the major spring snowmelt event, at multiple locations within each field (HRU), and compared with CRHM simulations. In cases of insufficient measured *SWE* data for estimation of $\sigma_{SWE}$, an alternative approach based on coefficients of variation representative of the landscape (Shook, 1995) could be used; it assumes that the snow cover can be approximated by a log-normal probability density function.

Although EOF flow and water quality observations were not available for the entire Steppler watershed, the hydrological model (CRHM) was set-up for the whole basin so that blowing snow transport between fields could be well represented. The basin was divided into 11 HRUs, each representing a distinct farm field (see Figure 4). This division is used to account for the dominant transport process in winter, that is, blowing snow, differences in farming practices, which may affect snow accumulation and ablation, and the location of the measuring stations for comparison with the model results.

Different modules in CHRM were used to account for (a) short-wave direct and diffuse solar radiation with adjustments for elevation and transmissivity (global module), (b) changes in snow albedo throughout the winter and during the melt period (Albedo module, after Gray and Landine, 1987), (c) transport and sublimation of blowing snow (pbsmSnobal module, after Pomeroy and Li, 2000), (d) the energy-budget during snowmelt, (Snobal module, after Marks, Kimball, Tingey, and Link, 1998), (e) evaporation using the Penman–Monteith method (evap module, after Armstrong, Pomeroy, and Martz, 2015), (f) infiltration in frozen and unfrozen grounds (Prairie Infiltration module, after Granger, Gray, and Dyck, 1984; Gray, Granger, and Landine, 1986), (g) soil moisture dynamics (Soil module, based on Fang et al., 2013), (h) crop growth (Grow_Crop module, after Armstrong, Pomeroy, and Martz, 2010), and (i) routing of surface and subsurface runoff using a lag and route method developed by Clark (1945) *Netroute* module, implemented by Pomeroy et al. (2007). A full description of CRHM and its modules is provided in Pomeroy et al. (2007).

WINTRA uses yearly measurements of premelt snow and fall soil $NO_3$ concentrations ($c_{snowpack}$ in Equation 8 and $c_{soil}$ in Equation 4, respectively). Unfortunately, the data measured do not cover the entire simulation period for all sites. Thus, the missing data were infilled using averages taken from the measured fields (Table 4). Soil chemistry data were available for $NO_3^- - N$. Soil samples were collected from the top 15-cm surface layer and analyzed using a potassium chloride extraction method (Gelderman & Beegle, 1998).

The performance of CRHM was evaluated through the model bias (MB) metric calculated for the premelt *SWE* and cumulative snowmelt runoff as:

$$MB = \frac{\sum X_{obs}}{\sum X_{mod}} - 1, \quad (9)$$

where $X_{obs}$ and $X_{mod}$ are the observed and simulated values, respectively. Positive and negative MB values implies model overprediction and under prediction, respectively. In the case of WINTRA, the available observed concentrations were insufficient to allow the estimation of cumulative loading, which is needed to apply the same MB metric used for flow. In this case, model predictions of rapid (subdaily) changes in runoff concentrations during snowmelt are of particular interest, and therefore, model results were compared to observations using the Nash–Sutcliffe efficiency (NSE) statistical measure computed using hourly data.

$$NSE = 1 - \frac{\sum (X_{obs} - X_{mod})^2}{(\sum X_{obs} - \mu_{obs})^2}, \quad (10)$$

where $X_{obs}$ and $X_{mod}$ are observed and simulated hourly values and $\mu_{obs}$ is the average of all observations. NSE values equal to one indicate a

**TABLE 4** Data available and used as model inputs in WINTRA

| Variable | | Field F3 | F4 | F7 | F9 | F10 | F11 |
|---|---|---|---|---|---|---|---|
| Snow | *SWE* | x | x | | | x | x |
| | $NO_3 + NO_2$ | x | x | | | x | x |
| Soil | N[a] | x | x | | | x | x |
| EOF | $NO_3 + NO_2$ | x | x | x | x | x | x |

*Note.* WINTRA = Winter Nutrient field Transport; EOF = edge-of-the-field.
[a]Samples taken from the top 5-cm soil layer.

perfect match between observations and model results, and NSE values equal to zero indicate model predictions as accurate as the mean of all observations.

## 3 | RESULTS

### 3.1 | Hydrological model

Figure 5 compares simulated and observed cumulative runoff and *SWE*. The model structure in CRHM is defined based on the understanding of the hydrological system (Pomeroy et al., 2007). Parameters are primarily physically based with empirical parameters based on extensive field observations in the region and therefore can be defined without the need for calibration. There is, of course, uncertainty in these parameters, but it has been shown to be relatively small compared to other approaches (e.g., Fang et al., 2013; MacDonald, Pomeroy, & Pietroniro, 2009; Pomeroy et al., 2007; Pomeroy et al., 2014).

The model shows good agreement with observations; it can capture well both *SWE* and runoff during conditions of both heavy snowfall and deep snowpacks (e.g., 2009) and reduced snowfall and shallow snowpacks (e.g., 2010). Results also show that the model can reproduce runoff responses from fields with very different drainage areas, for example, F4 (2.45 ha) and F7 (12.7 ha). Table 5 shows the estimated model bias (MB) for the different fields and years.

MB values for *SWE* range between −0.09 and 0.87, which implies 9% under prediction for F3 in 2009 and 87% overprediction for F10 in 2010. The medians of the positive and negative MB values are 0.17 and −0.05, respectively, suggesting a generally better prediction for most cases. MB values for runoff range between −0.28 and 0.74, which correspond to 28% under prediction for F7 in 2011 and 74% overprediction for F9 in 2010. As for *SWE*, the medians of the positive and negative MB values are much smaller, namely, 0.28 (28%) for overprediction and 0.04 (4%) for under prediction.

**TABLE 5** CRHM model bias (MB) test for total premelt snow water equivalent (*SWE*) and cumulative outflow

| Variable | Field | 2008 | 2009 | 2010 | 2011 |
|---|---|---|---|---|---|
| *SWE* | F3 | 0.07 | −0.09 | 0.42 | 0.61 |
| | F4 | 0.17 | −0.05 | – | 0.16 |
| | F7 | – | – | – | – |
| | F9 | – | – | – | – |
| | F10 | −0.05 | 0.24 | 1.04 | 0.08 |
| | F11 | 0.15 | 0.00 | 0.87 | 0.03 |
| Flow | F3 | – | – | 0.45 | −0.03 |
| | F7 | – | −0.07 | 0.07 | −0.27 |
| | F9 | – | −0.11 | 0.74 | −0.28 |
| | F10 | −0.01 | −0.01 | 0.31 | −0.03 |
| | F11 | −0.05 | −0.01 | 0.25 | 0.01 |

*Note.* CRHM = Cold Regions Hydrological Model.

### 3.2 | Nutrient model

Figure 6 compares observed and simulated $NO_3$ concentrations. Results are between 2009 and 2011, the period for which EOF runoff

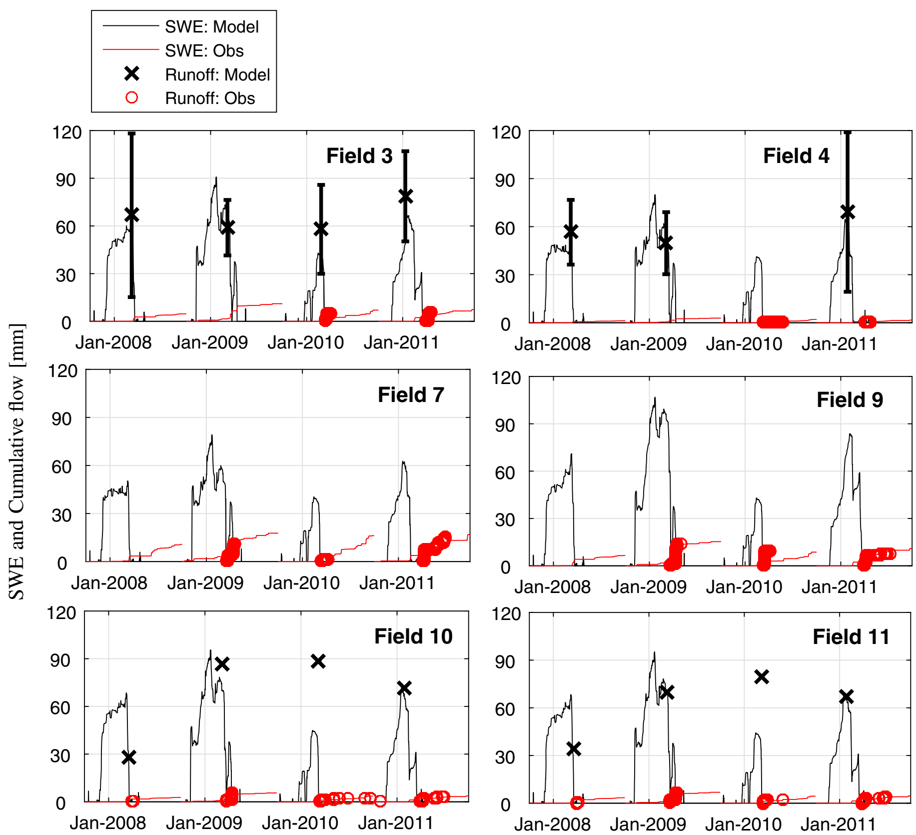


**FIGURE 5** Observed and simulated snow water equivalent (SWE) and edge-of-the-field (EOF) cumulative outflow

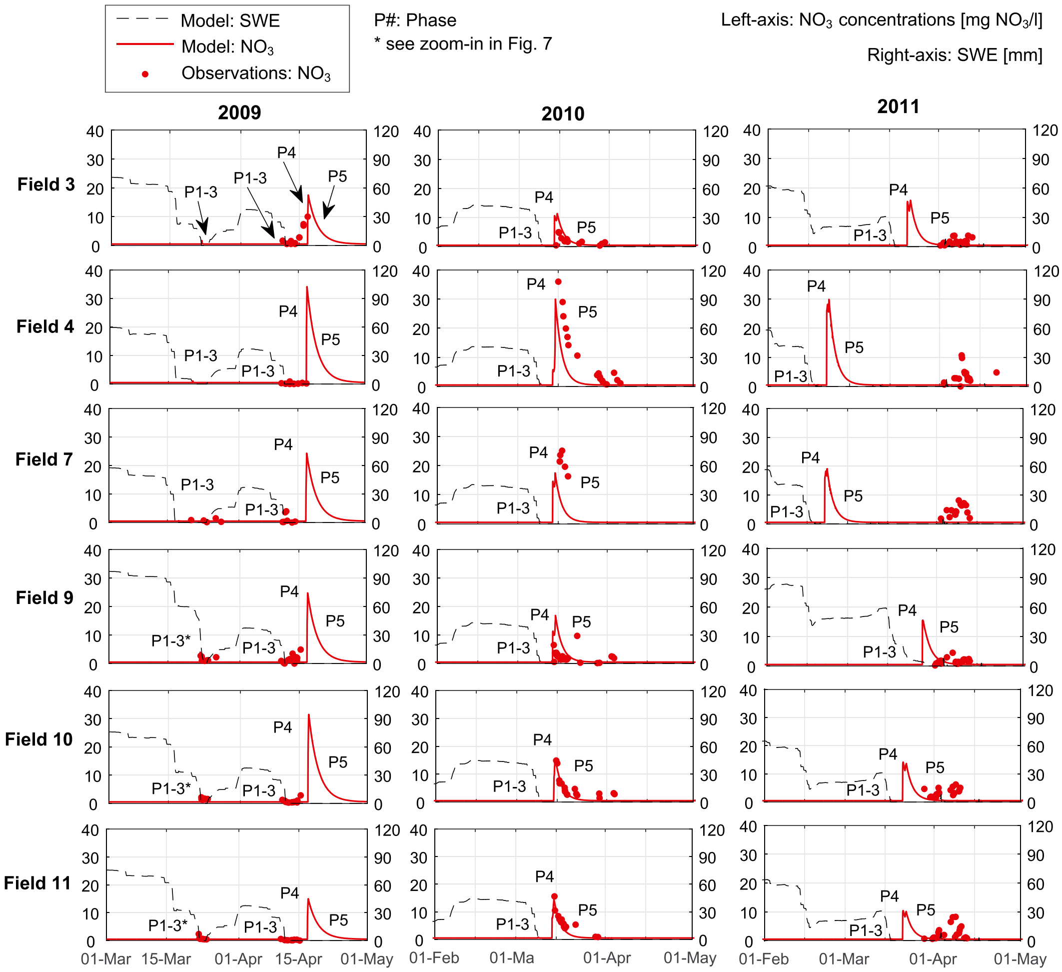


**FIGURE 6** Observed (red dots) and simulated (red solid line) edge-of-field $NO_3$ concentrations (left-axis) and *SWE* (black dashed line, right-axis)

concentrations were available. Results show a reasonably good model fit to the observed concentrations; the five-phase process, which is used in the conceptual model to account for changes in the dominant processes controlling runoff concentrations during snowmelt, can be identified in both the model and observations (P1 to P5 phases, in all panels of Figure 6).

*Phases 1–3*, which correspond to the initial period when the snow is the primary source of $NO_3$ (time characterized by a runoff ionic pulse caused by snow ion exclusion), were captured best in the 2009 observation data. Figure 7 shows in more detail observations and model results for this period. Unfortunately, observation data for this early period is limited to three fields in 2009, an issue that is discussed in Section 4.3. However, two peaks related to this phenomenon have been captured for each field; they occurred due to two consecutive snowmelt events during the spring of 2009; the one shown in Figure 7 corresponds to the first event (see more details in Section 5). The concentration peaks range between 4 mg $NO_3$/l in Field 9 and 2.5 mg $NO_3$/l in Field 11. These concentrations are smaller than those occurring at later stages in the melt when soil-runoff contact increases; 16 mg $NO_3$/l at both Fields 9 and 11 (Phase 3–4, Figure 6).

*Phases 3–4*, which is the period when the main nutrient source transitions from the snow to soil-pore water, is marked by a rapid increase in runoff concentrations as the thawing of snow and ice increases soil-runoff contact. This process is most visible in both observations and model results in the 2010 column panels. These peaks are followed by a rapid decrease in runoff $NO_3$ concentrations; concentrations drop to very low values in just a few hours or days.

Table 6 shows the calculated NSE efficiency. The performance of the model is generally satisfactory (median of NSE values is 0.32), although it varies significantly depending on the location and simulation period, for example, simulations are better for 2009 and 2010, than for 2011. NSE values vary between −7.03 for F10 in 2010 and 0.97 for F11 in 2009 (NSE values equal to one indicate a perfect match between observations and model results). NSE values computed for the whole basin show poorer model performance than when compared to most individual fields that is due to inferior model performance at some fields strongly affecting the NSE metric at basin scales. For example, although the 2009 model simulations show NSE values above 0.6 in 4 (out of 6) fields, the poor model performance in the remaining two fields (below 0.14) results in a lower NSE value for the basin (0.26).

## 4 | MODEL UNCERTAINTY

### 4.1 | Input data

The analysis in this section focuses on uncertainties in fall soil $NO_3$ concentration input data, although the role of uncertainties in the

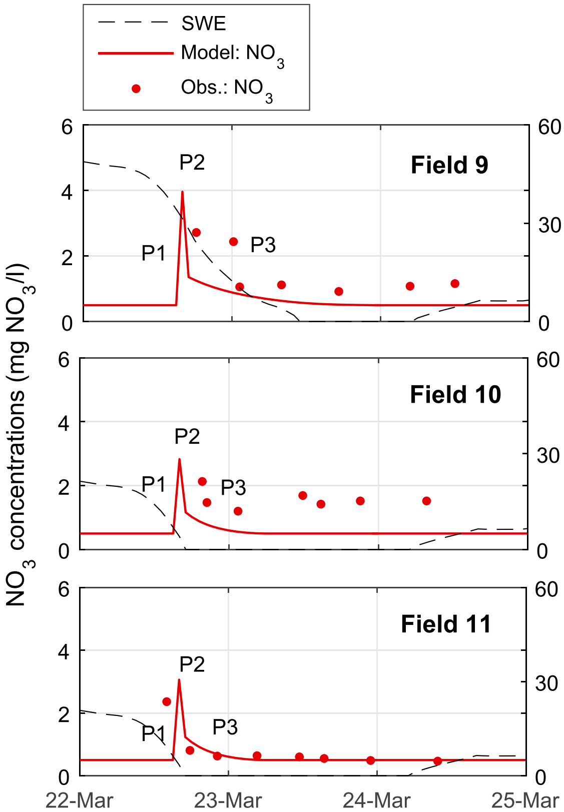


**FIGURE 7** Zoom-in to Phases 1–3 of snowmelt of 2009 to highlight early melt model results. Simulated (solid line) and observed (circles) runoff concentrations

**TABLE 6** Nash–Sutcliffe (*NSE*) efficiency for the water quality simulations using WINTRA

| Field | 2009 | 2010 | 2011 | All years |
|---|---|---|---|---|
| F3 | 0.14 | −1.15 | 0.48 | 0.03 |
| F4 | −2.08 | 0.40 | −1.20 | 0.23 |
| F7 | 0.76 | 0.24 | −3.17 | 0.13 |
| F9 | 0.63 | −7.03 | 0.60 | −1.92 |
| F10 | 0.91 | 0.81 | −3.94 | 0.43 |
| F11 | 0.97 | 0.76 | −0.36 | −0.11 |
| Basin | 0.26 | 0.20 | −0.48 | 0.02 |

*Note.* WINTRA = Winter Nutrient field Transport

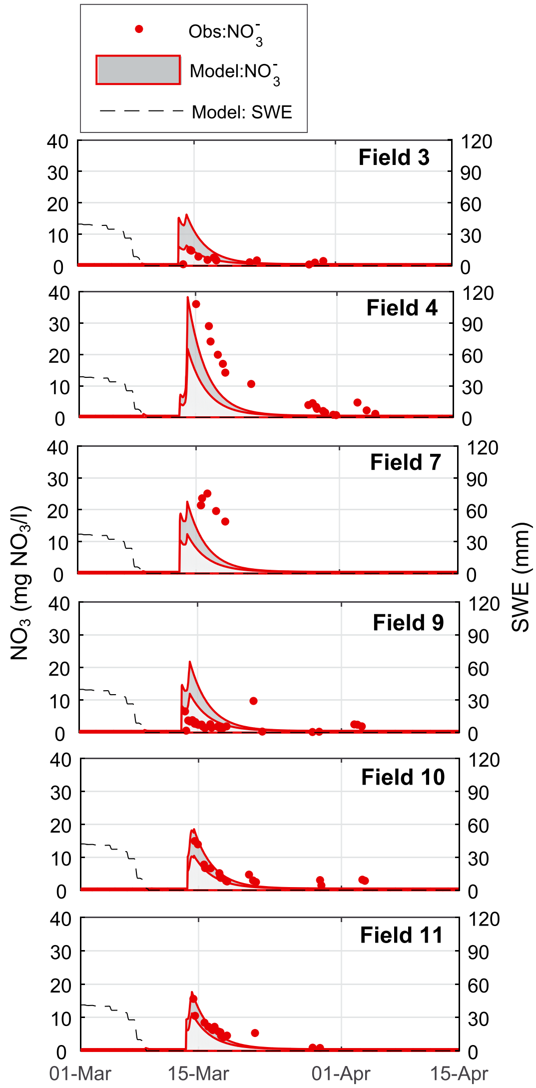


**FIGURE 8** Simulated (solid line) and observed (circles) edge-of-the-field (EOF) $NO_3$ concentrations (left-axis) and EOF cumulative runoff (dashed line, right-axis) taking into account the spatial standard deviation of the measured soil $NO_3$ concentrations used as model input

hydrological forcings computed by CRHM is recognized. Soil $NO_3$ concentrations play a critical role on seasonal load peaks, which occur between *Phases 3 and 4*. Thus, because the focus is the snowmelt period, these concentrations are reset in the model at the beginning of each hydrological year based on measurements taken in the fall. This approach allows bypassing the need for imprecise estimations of nutrient inputs during the growing season or fall, which would significantly increase simulation uncertainties. The $NO_3$ concentrations for each farm field (i.e., HRU) are calculated from multiple soil samples measured at different locations within each field to attempt to account for the heterogeneity in soil chemistry at the field-scale. Soil chemistry heterogeneity within each HRU is not considered further in the model computation. To assess the effect of this particular model simplification on WINTRA model output uncertainties, Figure 8 shows the model results obtained considering the spatial standard deviation (std) of the observed soil $NO_3$ concentrations as model inputs (i.e., model forced with *mean* ± *std* soil concentrations).

Results show that the measured EOF concentrations are typically within the range of possible model outputs when the variability in the measured soil $NO_3$ concentrations is considered in the model. In Fields 4 and 7, however, despite the concentration peaks being well represented by the model, there seems to be a lag between the model and observations. Although it is difficult to know with certainty, the reason for this delay in the observed runoff $NO_3$ concentration response, it is most likely related to local routing conditions and temporary storage, which can be caused by depressional storage, infiltration, and runoff over partially frozen soils and snow/ice dams.

The lowest observed concentration peaks are for Fields 3 and 9, which the model slightly overpredicts (see Panels in the 2010 column, Figure 6). These HRUs correspond to the agricultural fields subject to no tillage (Table 1) and no fertilizer application Roste 2015) in

2010. The decrease in runoff concentrations observed is, thus, possibly due to lower premelt soil $NO_3$ concentrations resulting from the absence of applied fertilizer or tillage disruption than can promote $NO_3$ release from aggregates (Elliott et al., 2001). Although reduced tillage can reduce loading of particulate nutrients and more mobile dissolved nutrients (Lal, 2003), stratification of less mobile nutrients such as phosphorous in the soil is a major concern that can be associated with increased export (Tiessen et al., 2010). The highest concentration peak is observed for Field 4, which is the field with the smallest drainage area (2.45 ha). This points to reduced time for concentration peak attenuations via dilution, routing, and lack of synchronicity; this effect is expected to be stronger for larger fields and as the water moves through the river network.

## 4.2 | Parameter calibration

The model uses two calibration parameters, namely, $k_d$ (Equation 4), a coefficient to account for soil solution $NO_3$ depletion via assimilation, denitrification, leaching, and runoff transport, and $k_l$ (Equation 8), which is a dimensionless leaching coefficient to compute preferential snow ion elution. Figure 9 shows the sensitivity of the model to these parameters. In the case of $k_d$, the values are computed for the entire simulation period, whereas in the case of $k_l$, NSE values are shown for 2009 as that was the year when concentration samples were available for the very initial period of melt, capturing the effect of snow ion elution.

Results show that the model is sensitive to both parameters. However, although it can capture the overall concentration dynamics well (see Section 3.2), the results presented in Panel (a) of Figure 9 show that $k_d$ parameter values, which were calibrated for the basin (i.e., all fields) and for the entire simulation period, produce poorer model performances. This is likely due to interannual and local (interfield) variabilities, probably caused by climate variability and human activities, being misrepresented by lumped model parameter calibrations. Field-specific and year-specific parameter calibrations within limits of data availability, or more explicit process representation, should be investigated in the future for continuous improvement of WINTRA. Model performance for $k_l$ (Panel b, Figure 9), which was also calibrated once for the entire basin and simulation period, was much improved; an expected outcome in this case due to the physical snow ion exclusion process relying on premelt snow concentrations and snow depth, variables that are explicitly represented in the model (see Equation 8 in Section 2.3).

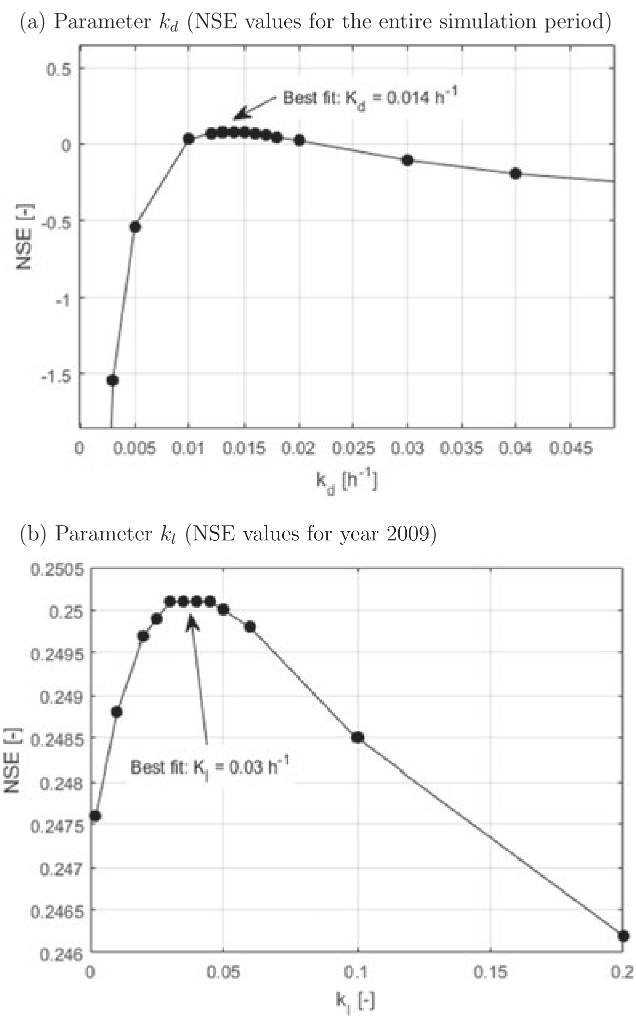


**FIGURE 9** Sensitivity of the model to (a) $k_d$ (Equation 4), coefficient to account for soil $NO_3$ depletion through runoff transport, and (b) $k_l$ (Equation 8), a dimensionless leaching coefficient to compute snow ion exclusion. NSE = Nash–Sutcliffe

## 4.3 | Model validation

Results show a reasonably good model fit to the observed concentrations; the model can adequately capture the overall runoff $NO_3$ dynamics, including the timing and magnitude of concentration peaks, for most HRUs. The five-phase hypothesis identified regarding the processes affecting runoff concentrations can be observed in both the model and observations. Results show, however, that the timing of the sampling did not always cover all phases for all fields. The melting period in the Canadian Prairies typically spans through relatively short time, that is, from a couple of days to 1–2 weeks, and runoff concentrations vary significantly and even more rapidly (e.g., time-scale of hours), especially in *Phase* 4 when soil-pore water $NO_3$ starts mixing with runoff. Unfortunately, the timing of the melting period is hard to anticipate, often resulting in limited time for deployment of field instrumentation.

Although the limited availability of observation data does not allow for a complete and extensive validation of the model for all years and fields, it is noteworthy that the peaks are generally accurately simulated without any parameter calibration—the only parameter affecting *Phase 4* is $k_d$, which is used to compute the loss of soil-pore water $NO_3$ only after the concentration peak has occurred. The decrease in runoff concentrations immediately following this peak are also adequately captured, which is also interesting given that it is controlled exclusively by that same parameter. It is important to note that the simulation of these rapid changes in runoff concentrations during snowmelt are possible due to CRHM–WINTRA coupled models computing hydrochemical changes at high temporal resolution, that is, hourly time steps.

## 5 | DISCUSSION

Modelling nutrient transport during snowmelt is a major scientific challenge. Runoff concentrations vary significantly during this period (e.g., Steinheimer et al., 1998) that suggests discontinuities in nutrient supply and changes in the dominant transport mechanisms (Liu et al., 2013). Research shows that existing nutrient models have a limited representation of relevant snow-related processes (e.g., snow fractionation, ion exclusion, and the impact of fractional snow-cover depletion on nutrient transport) and have seldom been tested in cold climates (Han et al., 2010). Continued work is thus necessary to improve simulation algorithms for this critical time and help reduce input data requirements and improve the efficiency of model parameter calibrations.

This research demonstrates the importance of adequate representation of key subdaily snow hydrological (e.g., snowpack disintegration) and biogeochemical/migration (e.g., preferential ion elution) processes in models for adequate simulation of the snowmelt period, a time marked by rapid and intense hydrological changes, and responsible for the main portion of the annual nutrient load to many rivers and lakes in Canada (e.g., Bourne et al., 2002). It also highlights the importance of subdaily monitoring and simulation for capturing strong nonlinear changes and discontinuities in nutrient supply and hydrological transport during this period. Given that most existing catchment nutrient models are run and compared with observations at weekly or monthly time intervals (Wellen et al., 2015), and many are unable to simulate single flood events (Arnold et al., 1998; Borah & Bera, 2003), our ability to simulate event-based transport remains a critical limitation in nutrient modelling. This challenge is particularly acute in snowmelt-dominated landscapes where the snowmelt period is often short, changes rapidly but is the dominant period of nutrient export.

The proposed model framework can accurately reproduce the observed $NO_3$ dynamics using the spatial and temporal distribution of SWE, simulated by CRHM, as the main hydrological driver. This suggests that other hydrological variables may play only a secondary role in runoff $NO_3$ at field-scales. During major spring snowmelt events, runoff and $NO_3$ concentrations strongly depend on melt processes and on the transitory distribution of snow and bare soil (Pomeroy et al., 1998), which is calculated in the model using the areal snow-cover fraction curve (*f*) computed independently for each field. Accounting for this process allowed capture of quick (i.e., subdaily) changes in soil-runoff contact and in soil $NO_3$ mobilization rates, which enabled the accurate simulation of the timing and magnitude of peak concentrations. Such processes and procedures are ignored in all nutrient models examined.

*Phases 1–5* were evident in both the observations and model results. During the initial stages of snowmelt (Phases 1–3), a peak in concentrations can be consistently observed in nearly every field, a phenomenon caused by snow fractionation and ion exclusion (e.g., Bales et al., 1989; Colbeck, 1981, 1987; Davies et al., 1987; Johannessen & Henriksen, 1978). These are promising results as snowmelt runoff ionic pulse computations have, to our knowledge, never been previously incorporated in long-term, continuous simulations in agricultural settings. Model and observations further suggest that such a process is typically followed by a drop in concentration as the ion enriched snow layers (i.e., upper layer and quasi-liquid layers within the snowpack) become depleted (Phases 1–2). The second but major load pulse occurs when the soil starts to uncover, due to soil-runoff contact increasing and soil-pore water $NO_3$ becoming more readily available for runoff transport (Phase 4). At last, in the final stages of the snowmelt event, when all snow has melted, the soil becomes the main and only source of $NO_3$. During this time, as the readily available portion of soil $NO_3$ solution is released to runoff (Phase 5), availability and runoff concentrations decline.

In some years, when major snowmelt events occur during winter and before the main (final) spring snowmelt event, such as observed in March 2009 and in February 2011 (see 2009 and 2011 panels in Figure 6), the ion enriched snow layers (Johannessen & Henriksen, 1978) may partially melt before spring and refreeze again within the snowpack or be transported via runoff over frozen or partially frozen soils with little infiltration. In these cases, the $NO_3$ shock load (Phases 1–3) is partially spent before the arrival of the actual spring freshet. This decreases the shock load during the second/final spring snowmelt. This is well captured in both observations

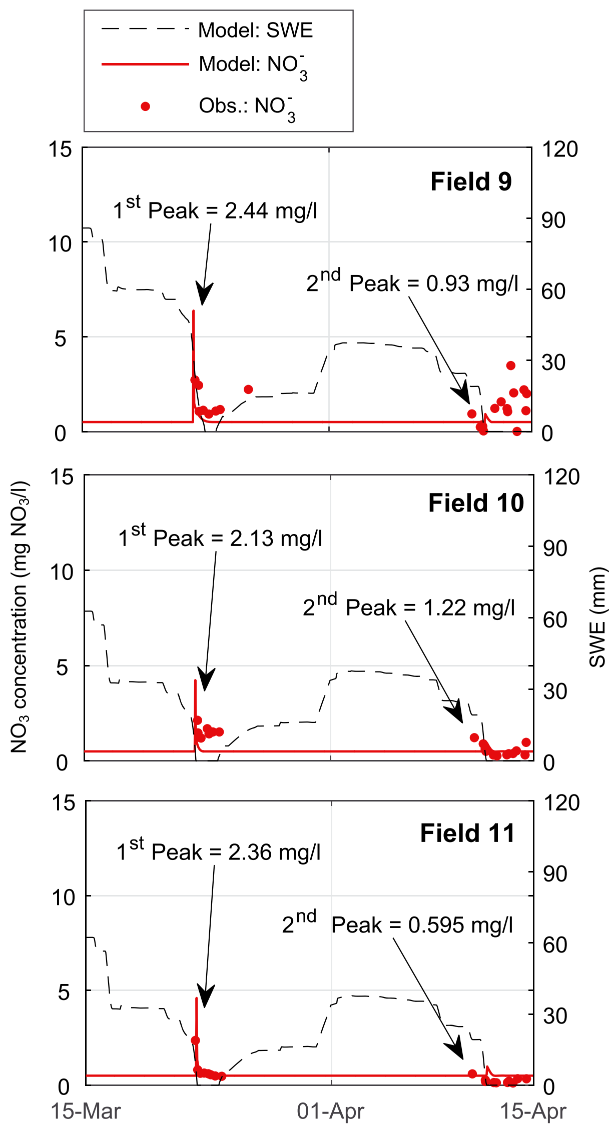


**FIGURE 10** Early release of snow ions during premature snowmelt in 2009

and model, as depicted in more detail in some examples in Figure 10. Such behaviour has been observed in two independent nutrient runoff experimental studies, one from Lac LaFlamme research watershed in Quebec (Jones & Pomeroy, 2001) and one from Central Sierra Snow Laboratory, Soda Springs, California, USA (Lee et al., 2008). However, this process is not represented in the suite of models examined here.

WINTRAs simulations do not include direct representation of N cycling processes of immobilization, nitrification, and denitrification. However, parameter $k_d[T^{-1}]$ is used to account for the lumped effect of these processes alongside with the flushing of surficial soil $NO_3$ during late snowmelt. More accurate representation of these processes can be important for precise modelling of nitrate production and consumption within agricultural environments (e.g., Clark et al., 2009; Snider et al., 2017; Steinheimer et al., 1998). The model assumes no runoff transport of soil $NO_3$ during early runoff due to the snow cover and soil frost limiting runoff-soil contact. It also considers that fall soil $NO_3$ is not transformed during winter. Soils in our study catchments undergo freezing, and although biological processes can occur at subzero temperatures, the good match between observations and model results may suggest that these processes are less important at these sites. The soils in these sites remain frozen through winter, have little free water, and may be expected to have low heterotrophic activity during winter and early snowmelt. During this period, soils in the catchment might be expected to have high N leaching and low microbial N retention (Brooks & Williams, 1999). However, mineralization, nitrification, and denitrification dynamics during winter and early snowmelt may have greater importance in areas with different snow cover and soil freezing dynamics (Brooks & Williams, 1999; Clark et al., 2009), although this requires assessment in agricultural environments. Next steps to support broad-scale application may require representation of the effects of freeze-thaw cycling on carbon substrate availability and microbial biomass and inclusion of under snow and snowmelt microbial processing. Balancing the need to represent key processes, with the common issue of overparameterization remains a key challenge in nutrient modelling. During the snowmelt period, more work in parallel linking model structure to nutrient processes and transport is merited to fill key knowledge gaps and integrate influential processes into numeric representations.

Analyses of the propagation of input observation data uncertainties in the model (i.e., soil fall concentration measurements) show that considering the spatial distribution of soil $NO_3$ concentrations within each HRU (i.e., field) can improve the model performance. This highlights the importance of adequate model spatial grid resolutions for accurate simulation of soil $NO_3$ concentration heterogeneity. It should be noted that in the case presented, as it is often the case, the discretization of the domain in HRUs was defined primarily for the hydrological model, CRHM, based on the hydrological response of the system, and less based on water quality considerations.

High frequency and spatial coverage data as available for this research are rare and, therefore, complementary methods for estimation of premelt snow and fall soil $NO_3$ concentrations (presently used as model inputs) or integration of WINTRA with larger scale (catchment) nutrient models may be necessary to broaden the application of the methodology proposed to basins with more limited monitoring data.

Finally, conventional process-based nutrient models are heavily parameterized despite their necessary simplification of physical and biogeochemical processes. One process that is often simulated relying heavily on parameters is the release and diffuse loading of snow and soil nutrients. The modelling framework proposed in this research provides an alternative high resolution (i.e., hourly) process-based estimation of such loading and transport patterns during snowmelt, one considering both physical and biochemical/migration processes unique to this period.

## 6 | CONCLUSIONS

A new process-based model that relies on snow physics, hydrological, and hydrochemical principles, in addition to generally observable snowmelt chemistry dynamics, WINTRA, was developed to simulate hourly $NO_3$ mobilization and field-scale transport in cold agricultural regions. Five distinct phases were identified during this brief but important and highly nonlinear transport period. These phases reflect the temporal dynamics arising from the composite nature of snow and soil, the nonuniform placement of $NO_3$ ions in the snowpack and prior to melt, and the complex interaction between snowmelt runoff and the mosaic of snow and bare soil patches that form as the snowpack disintegrates. In general, the snowmelt period is characterized by two main concentration peaks. The first one is smaller and occurs when an ion wavefront originating from ion-rich layers in the melting snowpack (i.e., upper layer and quasi-liquid layers) percolates through the snow along with the wetting front and reaches the field in-stream sampling locations. The second concentration peak is larger and occurs when the snow cover begins to disintegrate, and $NO_3$ in the melting soil-pore water starts to gradually mix with snowmelt runoff.

The simulations generally show a good agreement with observations (median of the NSE values of 0.32) and, although the performance of the model varies significantly depending on the location and simulation period (NSE values between 0.97 and −7.03), it demonstrates how field-scale runoff $NO_3$ concentrations result from the asynchronous release of snow and soil nutrients. It also shows that the relative contribution of snow and soil during snowmelt is subject to rapid changes and discontinuities, which require better, more explicit representation in catchment scale models for adequate simulation of runoff concentrations at suitable temporal resolutions (e.g., hourly).

CRHM-WINTRA provides a methodology for integration of physical and chemical elements on field-scale snowmelt $NO_3$ loading and transport estimations. Through modular coupling, for instance, the model can be transferred to existing catchment scale models for higher resolution and improved simulations during this period. Contrary to most nutrient models, both CRHM and WINTRA models require minimal calibration because they rely heavily on process representation and the understanding of the physical properties of the basin. One of the main current limitations of WINTRA is, however, the need for yearly inputs of premelt snow and fall soil $NO_3$ concentrations, an issue that should be addressed in the future for continuous improvement of the model.

This research established the importance of subdaily model resolution for adequate field-scale simulations, but its impact on larger (catchment) scale simulations should be assessed because damping of concentration pulses is expected to occur via dilution, routing, and lack of synchronicity as runoff water travels through the river network. Due to data constraints and to minimize the number of calibrated parameters in the model, the current version of WINTRA only simulates $NO_3$. Research effort should also be given to extending the model to other nitrogen species (e.g., ammonia, $NH_4$) and phosphorus (e.g., total dissolved phosphorus). This research would have to consider plant residues as an additional nutrient source and may necessitate the inclusion of complex processes such as redox changes during snowmelt and their influence on P release.

As a final remark, this work demonstrates how flexible, experimental tools like WINTRA, which rely heavily on observable data, can be used to improve nutrient models for cold regions. Uncertainty in forcing data is a widespread problem. Advances in model algorithms for this critical period of nutrient export will rely upon both the development of improved models with fine time steps that match the rapid changes during snowmelt, improved measurements of key forcing variables, and an understanding of geographic variation in links between snowmelt hydrology, chemistry, and biological processes.

## ACKNOWLEDGMENTS

The authors would like to thank the Canada Excellence Research Chair in Water Security, the Canada Research Chair in Water Resources and Climate Change, the Canadian Water Network and the Natural Sciences and Engineering Research Council (NSERC) through its CREATE in Water Security and Discovery grants (Grant 463960-2015) for financial support. We would like to extend our gratitude to Agriculture and Agri-Food Canada and Environment and Climate Change Canada for providing the data used in this study. Special thanks also to Xing Fang and Tom Brown of the Centre for Hydrology for helping setting up the CRHM model. Finally, this manuscript benefited greatly from the thoughtful comments of two anonymous reviewers.

## ORCID

*Diogo Costa* http://orcid.org/0000-0002-8841-2522

## REFERENCES


Arheimer, B., Dahné, J., Donnelly, C., Lindström, G., & Strömqvist, J. (2012). Water and nutrient simulations using the HYPE model for Sweden vs. the Baltic Sea basin influence of input-data quality and scale. *Hydrology Research*, *43*(4), 315–329.

Armstrong, R. N., Pomeroy, J. W., & Martz, L. W. (2015). Variability in evaporation across the Canadian Prairie region during drought and non-drought periods. *Journal of Hydrology*, *521*, 182–195.

Armstrong, R. N., Pomeroy, J. W., & Martz, L. W. (2010). Estimating evaporation in a prairie landscape under drought conditions. *Canadian Water Resources Journal*, *35*(2), 173–186.

Arnold, J. G., Muttiah, R. S., Srinivasan, R., & Allen, P. M (2000). Regional estimation of base flow and groundwater recharge in the Upper Mississippi River Basin. *Journal of Hydrology*, *227*(1), 21–40.

Arnold, J. G., Moriasi, D. N., Gassman, P. W., Abbaspour, K. C., White, M. J., Srinivasan, R., ... Jha, M. K. (2012). SWAT: Model use, calibration, and validation. *Trans. ASABE*, *55*(4), 1491–1508.

Arnold, J. G., Srinivasan, R., Muttiah, R. S., & Williams, J. R. (1998). Large area hydrologic modelling and assessment. Part I: Model development. *JAWRA Journal of the American Water Resources Association*, *34*(1), 73–89.

Bales, R. C., Davis, R. E., & Stanley, D. A. (1989). Ion elution through shallow homogeneous snow. *Water Resources Research*, *25*(8), 1869–1877.

Baulch, H. M., Elliott, J. A., Wilson, H. F., Cordeiro, M. R. C., & Flaten, D. N. (submitted). Soil and water management for nutrient control in the Northern Great Plains: A review. *Journal of Environmental Quality.*

Bechmann, M. E., Kleinman, P. J., Sharpley, A. N., & Saporito, L. S. (2005). Freeze-thaw effects on phosphorus loss in runoff from manured and catch-cropped soils. *Journal of Environment Quality*, *34*(6), 2301–2309.

Bicknell, B. R., Imhoff, J. C., Kittle Jr., J. L., Donigan Jr., A. S., & Johanson, R. C. (1997). Hydrological simulation program–Fortran, user's manual for version 11: U.S. environmental protection agency: National Exposure Research Laboratory, Athens, Ga., EPA/600/R-97/080, 755 p.

Borah, D., & Bera, M. (2003). SWAT model background and application reviews. In *2003 ASAE Annual International Meeting, American Society for Engineering in Agricultural, Food, and Biological Systems*, Las Vegas, Nevada, USA, pp. 1–16. https://doi.org/10.13031/2013.14000

Bourne, A., Armstrong, N., & Jones, G. (2002). A preliminary estimate of total nitrogen and total phosphorus loading to streams in Manitoba, Canada. (*Report No. 2002 - 04*): Manitoba Conservation.

Brooks, P. D., & Williams, M. W. (1999). Snowpack controls on nitrogen cycling and export in seasonally snow-covered catchments. *Hydrological Processes*, *13*(14-15), 2177–2190.

Brooks, P. D., Williams, M. W., & Schmidt, S. K. (1996). Microbial activity under alpine snowpacks, Niwot Ridge, Colorado. *Biogeochemistry*, *32*(2), 93–113.

Brunet, N. N., & Westbrook, C. J. (2012). Wetland drainage in the Canadian Prairies: Nutrient, salt and bacteria characteristics. *Agriculture, Ecosystems & Environment*, *146*(1), 1–12.

Buda, A. R., & Kleinman, P. J. A. (2009). Effects of hydrology and field management on phosphorus transport in surface runoff. *Journal of Environmental Quality*, *38*, 2273–2284.

Cade-Menun, B. J., Bell, G., Baker-Ismail, S., Fouli, Y., Hodder, K., McMartin, D. W., ... Wu, K. (2013). Nutrient loss from Saskatchewan cropland and pasture in spring snowmelt runoff. *Canadian Journal of Soil Science*, *93*(4), 445–458.

Casson, N. J., Eimers, M. C., & Watmough, S. A. (2012). Impact of winter warming on the timing of nutrient export from forested catchments. *Hydrological Processes*, *26*(17), 2546–2554.

Clark, C. O. (1945). Storage and the unit hydrograph. *Transactions of the American Society of Civil Engineers*, *110*(1), 1419–1446.

Clark, K., Chantigny, M. H., Angers, D. A., Rochette, P., & Parent, L. É. (2009). Nitrogen transformations in cold and frozen agricultural soils following organic amendments. *Soil Biology and Biochemistry*, *41*(2), 348–356.

Colbeck, S. C. (1981). A simulation of the enrichment of atmospheric pollutants in snow cover runoff. *Water Resources Research*, *17*(5), 1383–1388.

Colbeck, S. C. (1987). Snow metamorphism and classification. In Jones, H. G., & Orville-Thomas, W. J. (Eds.), *Seasonal Snowcovers: Physics, Chemistry, Hydrology*, Vol. *211* (pp. 1–35). Netherlands: Springer.

Corriveau, J., Chambers, P. A., & Culp, J. M. (2013). Seasonal variation in nutrient export along streams in the northern great plains. *Water, Air, and Soil Pollution*, *224*(7), 1594.

Davies, T. D., Brimblecombe, P., Tranter, M., Tsiouris, S., Vincent, C. E., Abrahams, P., & Blackwood, I. L. (1987). The Removal of Soluble Ions from Melting Snowpacks. In Jones, H. G., & Orville-Thomas, W. J. (Eds.), *Seasonal Snowcovers: Physics, Chemistry, Hydrology. NATO ASI Series (Series C: Mathematical and Physical Sciences)* (pp. 337–392). Netherlands, Dordrecht: Springer.

Davis, R. E. (1991). Links between snowpack physics and snowpack chemistry. In Davis, T. D., Tranter, M., & Jones, H. G. (Eds.), *Seasonal Snowpacks*, NATO ASI Series (Series G: Ecological Sciences), Vol. *28* (pp. 115–138). Berlin, Heidelberg: Springer.

Deelstra, J., Kværnø, S. H., Granlund, K., Sileika, A. S., Gaigalis, K., Kyllmar, K., & Vagstad, N. (2009). Runoff and nutrient losses during winter periods in cold climates requirements to nutrient simulation models. *Journal of Environmental Monitoring*, *11*(3), 602.

Douglas-Mankin, K. R., Srinivasan, R., & Arnold, J. G. (2010). Soil and water assessment tool (SWAT) model: Current developments and applications. *Trans. ASABE*, *53*(5), 1423–1431.

Duda, P. B., Hummel, P. R., Donigian Jr., A. S., & Imhoff, J. C. (2012). BASINS/HSPF: Model use, calibration, and validation. *Trans. ASABE*, *55*(4), 1523–1547.

ECCC (2014). Environment and climate change Canada: Historical climate data. Retrieved August, 2016. Available from: http://climate.weather.gc.ca.

Eimers, M. C., Watmough, S. A., Paterson, A. M., Dillon, P. J., & Yao, H. (2009). Long-term declines in phosphorus export from forested catchments in south-central Ontario. *Canadian Journal of Fisheries and Aquatic Sciences*, *66*(10), 1682–1692. https://doi.org/10.1139/F09-101

Elliott, J. (2013). Evaluating the potential contribution of vegetation as a nutrient source in snowmelt runoff. *Canadian Journal of Soil Science*, *93*(4), 435–443.

Elliott, J. A., Cessna, A. J., & Hilliard, C. R. (2001). Influence of tillage system on water quality and quantity in prairie pothole wetlands. *Canadian Water Resources Journal*, *26*(2), 165–181.

Essery, R., & Pomeroy, J. (2004). Implications of spatial distributions of snow mass and melt rate for snow-cover depletion: Observations in a subarctic mountain catchment. *Annals of Glaciology*, *38*, 195–201.

Fang, X., Pomeroy, J. W., Ellis, C. R., MacDonald, M. K., DeBeer, C. M., & Brown, T. (2013). Multi-variable evaluation of hydrological model predictions for a headwater basin in the Canadian Rocky Mountains. *Hydrology and Earth System Sciences*, *17*(4), 1635–1659.

Fuka, D. R., Easton, Z. M., Brooks, E. S., Boll, J., Steenhuis, T. S., & Walter, M. T. (2012). A simple process-based snowmelt routine to model spatially distributed snow depth and Snowmelt in the SWAT model. *JAWRA Journal of the American Water Resources Association*, *48*(6), 1151–1161.

Futter, M. N., Poste, A. E., Butterfield, D., Dillon, P. J., Whitehead, P. G., Dastoor, A. P., & Lean, D. R. S. (2012). Using the INCA-Hg model of mercury cycling to simulate total and methyl mercury concentrations in forest streams and catchments. *Science of the Total Environment*, *424*, 219–231.

Gelderman, R. H., & Beegle, D. (1998). Nitrate-nitrogen. In *Recommended chemical soil test procedures for the north central region*, North Central Regional Publ. 221 (Revised), Univ. of Missouri Agric. Exp. Stn., Columbia, pp. 17–21.

Glozier, N. E., Elliott, J. A., Holliday, B., Yarotski, J., & Harker, B. (2006). *Water quality characteristics and trends in a small agricultural watershed: South Tobacco Creek, Manitoba, 1992-2001*. Environment Canada, Ottawa, ON.

Granger, R. J., Gray, D. M., & Dyck, G. E. (1984). Snowmelt infiltration to frozen Prairie soils. *Canadian Journal of Earth Sciences*, *21*(6), 669–677.

Gray, D. M., Granger, R. J., & Landine, P. G. (1986). Modelling Snowmelt infiltration and runoff in a Prairie environment. In *Proceedings of the symposium: Cold regions hydrology*, pp. 427–438.

Gray, D. M., & Landine, P. G. (1987). Albedo model for shallow prairie snow covers. *Canadian Journal of Earth Sciences*, *24*(9), 1760–1768.

Gray, D. M., Norum, D. I., & Dyck, G. E. (1970). Densities of prairies snowpacks. In *Proc. 38th Annual Meeting Western Snow Conference*, pp. 24–30.

Gray, D. M., & Landine, P. G. (1988). An energy-budget snowmelt model for the Canadian Prairies. *Canadian Journal of Earth Sciences*, *25*(8), 1292–1303.

Groffman, P. M., Driscoll, C. D. T., Fahey, T. J., Hardy, J. P., Fitzhugh, R. D., Tierney, G. L., & Nolan, S. (2001). Effects of mild winter freezing on soil nitrogen and carbon dynamics in a northern hardwood forest. *Biogeochemistry*, *56*(2), 191–213.

Han, C. W., Xu, S. G., Liu, J. W., & Lian, J. J. (2010). Nonpoint-source nitrogen and phosphorus behavior and modeling in cold climate: A review. *Water Science and Technology*, *62*(10), 2277–2285. https://doi.org/10.2166/wst.2010.464

Hansen, N. C., Gupta, S. C., & Moncrief, J. F. (2000). Snowmelt runoff, sediment, and phosphorus losses under three different tillage systems. *Soil and Tillage Research*, *57*(1), 93–100.

Hansen, N. C., Sharpley, A. N., & Lemunyon, J. L. (2002). The fate and transport of phosphorus in agricultural systems. *Journal of Soil and Water Conservation*, *57*(6), 408–417.

Hodson, A. (2006). Biogeochemistry of snowmelt in an Antarctic glacial ecosystem. *Water Resources Research*, *42*(11), W11406. https://doi.org/10.1029/2005WR004311

Johannessen, M., & Henriksen, A. (1978). Chemistry of snow meltwater: Changes in concentration during melting. *Water Resources Research*, *14*(4), 615–619.

Jones, H. G. (1999). The ecology of snow-covered systems: A brief overview of nutrient cycling and life in the cold. *Hydrological Processes*, *13*(14-15), 2135–2147.

Jones, H. G., & Pomeroy, J. W. (2001). Early spring Snowmelt in a small boreal forest watershed: Influence of concrete frost on the hydrology and chemical composition of streamwaters during rain-on-snow events. In *58th Eastern Snow Conference*, pp. 209–218.

Krogh, S. A., Pomeroy, J. W., McPhee, J., Krogh, S. A., Pomeroy, J. W., & McPhee, J. (2015). Physically based mountain hydrological modeling using reanalysis data in Patagonia. *Journal of Hydrometeorology*, *16*(1), 172–193.

Lal, R. (2003). Global potential of soil carbon sequestration to mitigate the greenhouse effect. *Critical Reviews in Plant Sciences*, *22*(2), 151–184.

Lee, J., Nez, V. E., Feng, X., Kirchner, J. W., Osterhuber, R., & Renshaw, C. E. (2008). A study of solute redistribution and transport in seasonal snowpack using natural and artificial tracers. *Journal of Hydrology*, *357*(3), 243–254.

Li, S., Elliott, J. A., & Tiessen, K. H. D. (2011). The effects of multiple beneficial management practices on hydrology and nutrient losses in a small watershed in the Canadian Prairies. *Journal of Environmental Quality*, *40*(5), 1627–1642.

Lilbæk, G. (2007). Compositional change of meltwater infiltrating frozen ground. Retrieved from http://hdl.handle.net/10388/etd-03312009-101916. (Ph.D. Thesis).

Lilbæk, G., & Pomeroy, J. W. (2008). Ion enrichment of snowmelt runoff water caused by basal ice formation. *Hydrological Processes*, *22*(15), 2758–2766.

Lilbæk, G., & Pomeroy, J. W. (2010). Laboratory evidence for enhanced infiltration of ion load during snowmelt. *Hydrology and Earth System Sciences*, *14*(7), 1365–1374.

Lindström, G., Pers, C., Rosberg, J., Strömqvist, J., & Arheimer, B. (2010). Development and testing of the HYPE (Hydrological Predictions for the Environment) water quality model for different spatial scales. *Hydrology Research*, *41*(3-4), 295.

Lipiec, J., Kuś, J., Słowińska-Jurkiewicz, A., & Nosalewicz, A. (2006). Soil porosity and water infiltration as influenced by tillage methods. *Soil and Tillage Research*, *89*(2), 210–220.

Liu, K., Elliott, J. A., Lobb, D. A., Flaten, D. N., & Yarotski, J. (2013). Critical factors affecting field-scale losses of nitrogen and phosphorus in spring snowmelt runoff in the Canadian Prairies. *Journal of Environment Quality*, *42*(2), 484.

Liu, K., Elliott, J. A., Lobb, D. A., Flaten, D. N., & Yarotski, J. (2014). Nutrient and sediment losses in snowmelt runoff from perennial forage and annual cropland in the Canadian Prairies. *Journal of Environment Quality*, *43*(5), 1644.

López-Moreno, J. I., Boike, J., Sanchez-Lorenzo, A., & Pomeroy, J. W. (2016). Impact of climate warming on snow processes in Ny-Ålesund, a polar maritime site at Svalbard. *Global and Planetary Change*, *146*, 10–21.

López-Moreno, J. I., Revuelto, J., Gilaberte, M., Morán-Tejeda, E., Pons, M., Jover, E., ... Pomeroy, J. W. (2014). The effect of slope aspect on the response of snowpack to climate warming in the Pyrenees. *Theoretical and Applied Climatology*, *117*(1-2), 207–219.

LWST, Lake Winnipeg Stewardship Board (2009). Manitoba's progress towards implementing recommendations of the Lake Winnipeg Stewardship Board: A report to the Minister of Water Stewardship. (*Tech. rep.*): Lake Winnipeg Stewardship Board.

MacDonald, M. K., Pomeroy, J. W., & Pietroniro, A. (2009). Parameterizing redistribution and sublimation of blowing snow for hydrological models: Tests in a mountainous subarctic catchment. *Hydrological Processes*, *23*(18), 2570–2583.

Mahmood, T. H., Pomeroy, J. W., Wheater, H. S., & Baulch, H. M. (2016). Hydrological responses to climatic variability in a cold agricultural region. *Hydrological Processes*, *31*(4), 845–870.

Marks, D., Kimball, J., Tingey, D., & Link, T. (1998). The sensitivity of snowmelt processes to climate conditions and forest cover during rain-on-snow: A case study of the 1996 Pacific Northwest flood. *Hydrological Processes*, *12*(10-11), 1569–1587.

Marsh, P., & Pomeroy, J. W. (1996). Meltwater fluxes at an Arctic forest-tundra site. *Hydrological Processes*, *10*(10), 1383–1400.

Marsh, P., & Pomeroy, J. W. (1999). Spatial and temporal variations in snowmelt runoff chemistry, Northwest Territories, Canada. *Water Resources Research*, *35*(5), 1559–1567.

Marsh, P., & Woo, M.-K. (1984). Wetting front advance and freezing of meltwater within a snow cover: 1. Observations in the Canadian Arctic. *Water Resources Research*, *20*(12), 1853–1864.

Martius, C., Rudenko, I., Lamers, J. P. A., & Vlek, P. L. G. (2011). *Cotton, water, aalts and soums: Economic and ecological restructuring in Khorezm, Uzbekistan*: Springer Science & Business Media.

McIntyre, N., Jackson, B., Wade, A. J., Butterfield, D., & Wheater, H. S. (2005). Sensitivity analysis of a catchment-scale nitrogen model. *Journal of Hydrology*, *315*(1), 71–92.

Mekonnen, B. A., Mazurek, K. A., & Putz, G. (2016). Incorporating landscape depression heterogeneity into the Soil and Water Assessment Tool (SWAT) using a probability distribution. *Hydrological Processes*, *30*(13), 2373–2389.

Mekonnen, B. A., Mazurek, K. A., & Putz, G. (2017). Modeling of nutrient export and effects of management practices in a cold-climate prairie watershed: Assiniboine River Watershed, Canada. *Agricultural Water Management*, *180*, 235–251.

Messiga, A. J., Ziadi, N., Morel, C., & Parent, L.-E. (2010). Soil phosphorus availability in no-till versus conventional tillage following freezing and thawing cycles. *Canadian Journal of Soil Science*, *90*(3), 419–428.

Meyer, T., & Wania, F. (2008). Organic contaminant amplification during snowmelt. *Water Research*, *42*(8-9), 1847–1865.

Miller, M. H., Beauchamp, E. G., & Lauzon, J. D. (1994). Leaching of nitrogen and phosphorus from the biomass of three cover crop species. *Journal of Environmental Quality*, *23*(2), 267–272.

Moog, D. B., & Whiting, P. J. (2002). Climatic and agricultural factors in nutrient exports from two watersheds in Ohio. *Journal of Environmental Quality*, *31*(2), 72–83.

Nicholaichuk, W. (1967). Comparative watershed studies in southern Saskatchewan. *Trans. ASAE*, *10*, 502–504.

Ofukany, A. F. A., Hobson, K. A., Wassenaar, L. I., & Bond, A. L. (2015). Prey consumption and trace element concentrations in double-crested cormorants (Phalacrocorax auritus) from Lake Winnipeg, Canada. *Journal of Great Lakes Research*, *41*(2), 643–651.

Panuska, J. C., Karthikeyan, K. G., & Norman, J. M. (2008). Sediment and phosphorus losses in snowmelt and rainfall runoff from three corn management systems. *Transactions of the ASABE 51.1*, 95–105.

Pellerin, B. A., Saraceno, J. F., Shanley, J. B., Sebestyen, S. D., Aiken, G. R., Wollheim, W. M., & Bergamaschi, B. A. (2012). Taking the pulse of snowmelt: In situ sensors reveal seasonal, event and diurnal patterns of nitrate and dissolved organic matter variability in an upland forest stream. *Biogeochemistry*, *108*(1-3), 183–198.

Petrone, K., Buffam, I., & Laudon, H. (2007). Hydrologic and biotic control of nitrogen export during snowmelt: A combined conservative and reactive tracer approach. *Water Resources Research*, *43*(6), W06420. https://doi.org/10.1029/2006WR005286

Piatek, K. B., Mitchell, M. J., Silva, S. R., & Kendall, C. (2005). Sources of nitrate in snowmelt discharge: Evidence from water chemistry and stable isotopes of nitrate. *Water, Air, and Soil Pollution*, *165*(1-4), 13–35.

Pomeroy, J. W., Davies, T. D., & Tranter, M. (1991). The Impact of Blowing Snow on Snow Chemistry, *Seasonal snowpacks: Processes of compositional change*. Berlin, Heidelberg: Springer, pp. 71–113.

Pomeroy, J. W., Gray, D. M., Brown, T., Hedstrom, N. R., Quinton, W. L., Granger, R. J., & Carey, S. K. (2007). The cold regions hydrological model: A platform for basing process representation and model structure on physical evidence. *Hydrological Processes*, *21*(19), 2650–2667.

Pomeroy, J. W., Gray, D. M., Shook, K. R., Toth, B., Essery, R. L. H., Pietroniro, A., & Hedstrom, N. (1998). An evaluation of snow accumulation and ablation processes for land surface modelling. *Hydrological Processes*, *12*(15), 2339–2367.

Pomeroy, J. W., & Jones, H. G. (1996). Wind-blown snow: Sublimation, transport and changes to polar snow, *Chemical exchange between the atmosphere and polar snow*. Berlin, Heidelberg: Springer, pp. 453–489.

Pomeroy, J. W., Jones, H. G., Tranter, M., & Lilbæk, G. (2006). Hydrochemical processes in snow-covered basins. *Encyclopedia of Hydrological Sciences*, *14*, 163.

Pomeroy, J. W., & Li, L. (2000). Prairie and arctic areal snow cover mass balance using a blowing snow model. *Journal of Geophysical Research*, *105*(D21), 26619–26634.

Pomeroy, J. W., Shook, K., Fang, X., Dumanski, S., Westbrook, C., & Brown, T. (2014). Improving and testing the prairie hydrological model at Smith Creek Research Basin. Centre for Hydrology Report #14. (*Tech. rep.*)

Quinton, W. L., & Pomeroy, J. W. (2006). Transformations of runoff chemistry in the Arctic tundra, Northwest Territories, Canada. *Hydrological Processes*, *20*(14), 2901–2919.

Rasouli, K., Pomeroy, J. W., & Marks, D. G. (2015). Snowpack sensitivity to perturbed climate in a cool mid-latitude mountain catchment. *Hydrological Processes*, *29*(18), 3925–3940.

Rattan, K. J., Corriveau, J. C., Brua, R. B., Culp, J. M., Yates, A. G., & Chambers, P. A. (2017). Quantifying seasonal variation in total phosphorus and nitrogen from prairie streams in the Red River Basin, Manitoba Canada. *Science of The Total Environment*, *575*, 649–659.

Roste, J. (2015). Development and evaluation of a Canadian Prairie Nutrient Transport Model. Retrieved from http://hdl.handle.net/10388/ETD-2015-07-2172. (MS.c. thesis.), University of Saskatchewan.

Schindler, D. W., Hecky, R. E., & McCullough, G. K. (2012). The rapid eutrophication of Lake Winnipeg: Greening under global change. *Journal of Great Lakes Research*, *38*(Supplement 3), 6–13.

Sebestyen, S. D., Boyer, E. W., Shanley, J. B., Kendall, C., Doctor, D. H., Aiken, G. R., & Ohte, N. (2008). Sources, transformations, and hydrological processes that control stream nitrate and dissolved organic matter concentrations during snowmelt in an upland forest. *Water Resources Research*, *44*(12), W12410. https://doi.org/10.1029/2008WR006983

Shirmohammadi, A., Chu, T. W., Montas, H., & Sohrabi, T. (2001). SWAT model and its applicability to watershed nonpoint-source pollution assessment. In *ASAE Annual Meeting, Sacramento, California, Paper no. 01-2005*, pp. 1–26.

Shook, K. R. (1995). Simulation of the ablation of prairie snowcovers. (Ph.D. Thesis), University of Saskatchewan.

Shook, K. R., & Pomeroy, J. W. (2011). Memory effects of depressional storage in Northern Prairie hydrology. *Hydrological Processes*, *25*(25), 3890–3898.

Shrestha, R. R., Dibike, Y. B., & Prowse, T. D. (2012). Modeling climate change impacts on hydrology and nutrient loading in the upper assiniboine catchment. *JAWRA Journal of the American Water Resources Association*, *48*(1), 74–89.

Snider, D. M., Wagner-Riddle, C., & Spoelstra, J. (2017). Stable isotopes reveal rapid cycling of soil nitrogen after manure application. *Journal of Environment Quality*, *46*(2), 261.

Spence, C., Guan, X. J., Phillips, R., Hedstrom, N., Granger, R., & Reid, B. (2010). Storage dynamics and streamflow in a catchment with a variable contributing area. *Hydrological Processes*, *24*(16), 2209–2221.

Spence, C., Guan, X. J., Phillips, R., Hedstrom, N., Granger, R., & Reid, B. (2009). Storage dynamics and streamflow in a catchment with a variable contributing area. *Hydrological Processes*, *24*(16), 2209–2221.

Stein, J., Jones, H. G., Roberge, J., & Sochanska, W. (1986). The prediction of both runoff quality and quantity by the use of an integrated snowmelt model. *IAHS-AISH publication*, *155*, 347–358.

Stein, J., Proulx, S., & Lévesque, D. (1994). Forest floor frost dynamics during spring snowmelt in a boreal forested basin. *Water Resources Research*, *30*(4), 995–1007.

Steinheimer, T. R., Scoggin, K. D., & Kramer, L. A. (1998). Agricultural chemical movement through a field-size watershed in Iowa: Surface hydrology and nitrate losses in discharge. *Environmental Science and Technology*, *32*(8), 1048–1052.

Tiessen, K. H. D., Elliott, J. A., Yarotski, J., Lobb, D. A., Flaten, D. N., & Glozier, N. E. (2010). Conventional and conservation tillage: Influence on seasonal runoff, sediment, and nutrient losses in the Canadian Prairies. *Journal of Environment Quality*, *39*(3), 964.

Tobin, C., Schaefli, B., Nicótina, L., Simoni, S., Barrenetxea, G., Smith, R., ... Rinaldo, A. (2013). Improving the degree-day method for sub-daily melt simulations with physically-based diurnal variations. *Advances in Water Resources*, *55*, 149–164.

Townsend-Small, A., McClelland, J. W., Max H., R., & Peterson, B. J. (2011). Seasonal and hydrologic drivers of dissolved organic matter and nutrients in the upper Kuparuk River, Alaskan Arctic. *Biogeochemistry*, *103*(1-3), 109–124.

Tranter, M., Brimblecombe, P., Davies, T. D., Vincent, C. E., Abrahams, P. W., & Blackwood, I. (1986). The composition of snowfall, snowpack and meltwater in the Scottish highlands-evidence for preferential elution. *Atmospheric Environment (1967)*, *20*(3), 517–525.

Tranter, M., & Jones, H. G. (2001). The Chemistry of Snow: Processes and Nutrient Cycling. In Jones, H. G., Pomeroy, J. W., Walker, A. D., & Hoham, R. W. (Eds.), *Snow ecology: An interdisciplinary examination of snow-covered ecosystems* (pp. 378). New York: Cambridge University Press.

Voora, V., & Venema, H. D. (2009). An ecosystem services assessment of the Lake Winnipeg Watershed: Phase 1 report southern Manitoba analysis. (Tech. Rep.) Funded by Environment Canada - Policy Development Division International Institute for Sustainable Development.

Wade, A. J., Whitehead, P. G., & O'Shea, L. C. M. (2002). The prediction and management of aquatic nitrogen pollution across Europe: An introduction to the Integrated Nitrogen in European Catchments project (INCA). *Hydrology and Earth System Sciences*, *6*(3), 299–3.

Weber, M., Bernhardt, M., Pomeroy, J. W., Fang, X., Härer, S., & Schulz, K. (2016). Description of current and future snow processes in a small basin in the Bavarian Alps. *Environmental Earth Sciences*, *75*(17), 1223.

Wellen, C., Arhonditsis, G. B., Labencki, T., & Boyd, D. (2014). Application of the SPARROW model in watersheds with limited information: A bayesian assessment of the model uncertainty and the value of additional monitoring. *Hydrological Processes*, *28*(3), 1260–1283.

Wellen, C., Kamran-Disfani, A. R., & Arhonditsis, G. B. (2015). Evaluation of the current state of distributed watershed nutrient water quality modeling. *Environmental Science and Technology*, *49*(6), 3278–3290.

Whitehead, P. G., Wilson, E. J., Butterfield, D., & Seed, K. (1998). A semi-distributed integrated flow and nitrogen model for multiple source assessment in catchments (INCA): Part II—Application to large river basins in south Wales and eastern England. *Science of the Total Environment*, *210-211*, 559–583.

Whitehead, P. G., Wilson, E. J., Butterfield, D., & Seed, K. (1998). A semi-distributed ntegrated itrogen model for multiple source assessment in tchments (INCA): Part I model structure and process equations. *Science of The Total Environment*, *210-211*, 547–558.

Williams, M. W., & Melack, J. M. (1991). Solute chemistry of snowmelt and runoff in an Alpine Basin, Sierra Nevada. *Water Resources Research*, *27*(7), 1575–1588.

Wren, S. N., & Donaldson, D. J. (2011). Exclusion of nitrate to the airice interface during freezing. *The Journal of Physical Chemistry Letters*, *2*(16), 1967–1971.

X. Wang, X., A. M., & Melesse, A. M. (2005). Evaluation of the SWAT model's snowmelt hydrology in a northwestern Minnesota watershed. *Trans. ASAE*, *48*(4), 1359–1376.

Zhang, D., Chen, X., & Yao, H. (2016). SWAT-CSenm: Enhancing SWAT nitrate module for a Canadian Shield catchment. *Science of the Total Environment*, *550*, 598–610.

Zou, H., Zhu, J., Zhou, L., Li, P., & Ma, S. (2014). Validation and application of reanalysis temperature data over the Tibetan Plateau. *Acta Meteorologica Sinica*, *28*(1), 139–149.

**How to cite this article:** Costa D, Roste J, Pomeroy J, et al. A modelling framework to simulate field-scale nitrate response and transport during snowmelt: The WINTRA model. *Hydrological Processes*. 2017;31:4250–4268. https://doi.org/10.1002/hyp.11346